

THE QUENAST PLUG: A MEGA-PORPHYROCLAST DURING THE BRABANTIAN OROGENY (SENNE VALLEY, BRABANT MASSIF)

Timothy N. DEBACKER¹ & Manuel SINTUBIN²

(11 figures, 3 tables)

1. Research Unit Palaeontology, Geology & Pedology, Universiteit Gent, Krijgslaan 281, S8, B-9000 Gent, E-mail: Timothy.Debacker@UGent.be

2. Geodynamics & Geofluids Research Group, Katholieke Universiteit Leuven, Celestijnenlaan 200E, B-3001 Leuven, E-mail: Manuel.Sintubin@Geo.kuleuven.be

ABSTRACT. In the fine-grained Ordovician siliciclastic deposits surrounding the Quenast plug, a variety of structural features demonstrate that the Quenast plug was emplaced prior to the Brabantian deformation event. These features include: a) a large-scale bending of the cleavage, mimicking the shape of the plug; b) a concomitant change in the orientation of the transverse fractures; c) a marked variation in cleavage intensity around the plug, with a high-strain zone along the NE-side of the plug and a low-strain zone along the NW-side of the plug; d) contractional and dilational kink bands. In combination with the ellipsoidal cross-section of the plug, these features indicate that the Quenast plug can be regarded as having acted as a mega-porphyroclast during the Brabantian deformation event.

The different structural features are discussed and related to the geometry and deformation of the Quenast plug. Also the temporal and spatial relationships of the Quenast plug with respect to the Asquempont Detachment System and the Nieuwpoort-Asquempont Fault Zone are discussed. Finally, a preliminary attempt is made at estimating the shortening across the plug. Future work, concentrating on the magnetic fabric within the plug, will shed further light on the behaviour of the plug during the Brabantian deformation event.

KEYWORDS: Anglo-Brabant Deformation Belt, cleavage, Nieuwpoort-Asquempont Fault Zone, strain, X-ray pole figure goniometry

1. Introduction

Together with the Sennette valley, the Senne valley forms one of the classical outcrop areas of the Brabant Massif (cf. Galeotti, 1835; de Collegno, 1835; Dumont, 1848; de la Vallée Poussin & Renard, 1876). The long-time geological interest in the Senne valley can largely be attributed to the quartz microdiorite plug at Quenast (Fig. 1). Although the intrusive nature of this magmatic body was already suggested 166 years ago (Galeotti, 1835; cf. de la Vallée Poussin & Renard, 1876; Corin, 1965), its age remained unknown for a long time (cf. Galeotti, 1835; Dumont, 1848; Malaise, 1873; Jedwab, 1950; Corin, 1965). Finally, André & Deutsch (1984) obtained a U-Pb zircon age of 433 ± 10 Ma for the emplacement of the Quenast plug. This age ranges from the base of the Llandovery to the top of the Wenlock in the time-scale of Gradstein & Ogg (1996), and from the middle Hirnantian to the basal Ludfordian (upper Ludlow) according to the time-scale of Gradstein *et al.* (2004). This time interval clearly predates the Givetian angular unconformity at the southern rim of the Brabant Massif (e.g. Legrand, 1967; Van Grootel *et al.*, 1997), and hence suggests a pre-kinematic (pre-Brabantian) emplacement of the Quenast plug (André & Deutsch, 1984). However, this absolute age interval partly overlaps with the recently proposed late Llandovery – late Emsian(-Eifelian?) time interval for the long-lived Brabantian Orogeny (Debacker *et al.*,

2005a). In addition, according to the aforementioned time-scales, the stratigraphic age of the volcanic rocks of the late Caradoc – early Ashgill Madot Formation in the Fauquez area (Vanmeirhaeghe *et al.*, 2005, Verniers *et al.*, 2005), sometimes regarded as being derived from the Quenast plug (André, 1991b), is considerably older than 433 ± 10 Ma. Because of these considerations, in order to be convincing, the pre-kinematic origin of the Quenast plug suggested by the absolute ages should be checked and should be backed-up by structural outcrop data.

As a consequence of the huge exposures caused by the open-pit mining of the Quenast microdiorite plug, numerous studies have been performed. However, although these gave important information regarding the age, petrology and geochemistry of the magmas (André & Deutsch, 1984; André, 1991b; cf. André, 1991a), the few structural studies yielded little result. Moreover, judging from published structural field observations, there appears to be no agreement on whether or not the Quenast plug was emplaced prior to the Brabantian Orogeny. An analysis of the fracture orientations in the plug lead Jedwab (1950) to conclude a late-syntectonic to post-tectonic, Early Devonian origin of the plug. In contrast, Corin (1965) mentions a curvature of the Lower Palaeozoic rocks around the magmatic bodies at Quenast and at Bierghes (“as if these bodies acted as stable blocs during the deformation”), thus suggesting a pre-tectonic age.

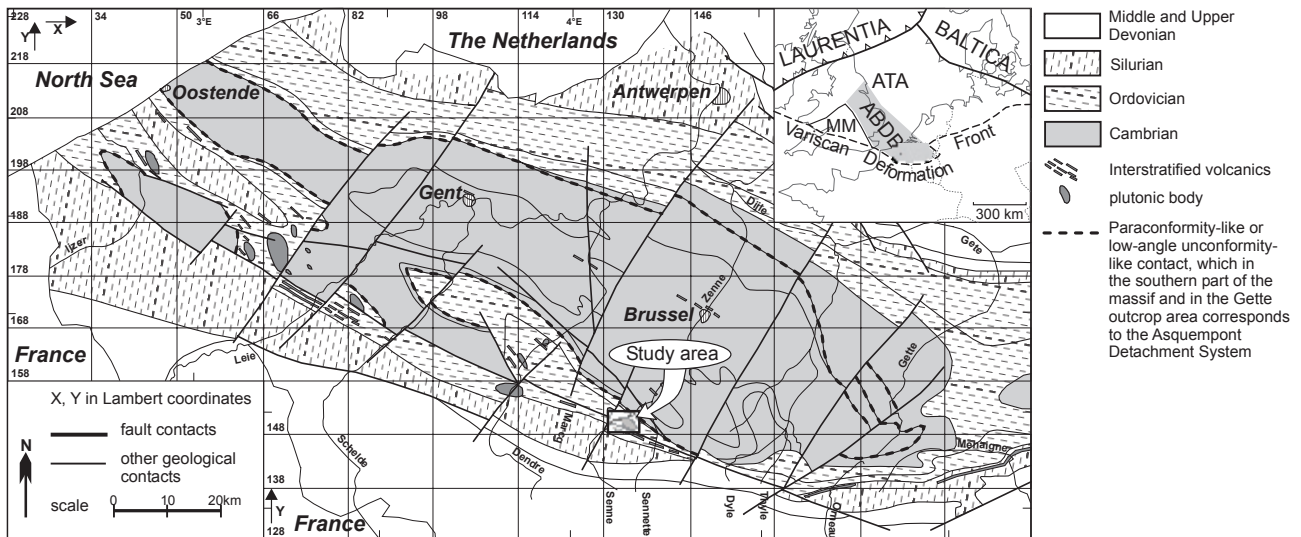


Figure 1 : Geological subcrop map of the Brabant Massif, after De Vos *et al.* (1993) and Van Grootel *et al.* (1997), with location of the study area (see also Fig. 2) and position of the Brabant Massif within Avalonia, as the southeastern part of the Anglo-Brabant Deformation Belt (ABDB), flanking the Midlands Microcraton (MM) (upper right inset).

Taking into account the poor results of the previous structural studies inside the magmatic body, possibly caused by the competence of the rock and the difficulties in distinguishing cooling fractures and flow banding from tectonic features (cf. Jedwab, 1950), this study will focus on the direct surroundings of the Quenast plug. Several kinematic features are preserved in the fine-grained incompetent host rocks, which can be used to study the possible influence of the intrusive body on the deformation geometry, and thus allow an independent examination of the pre-kinematic emplacement age suggested by the U-Pb zircon ages.

2. Geological setting and lithostratigraphy

The Quenast plug is a quartz microdiorite situated in the southern part of the single-phase deformed Brabant Massif

(Anglo-Brabant Deformation Belt; Fig. 1). This microdiorite has an ellipsoidal cross-section (long axis ~1.6 km, short axis ~1.3 km) and is interpreted as a steeply NE-plunging feeder pipe or volcano neck (Fig. 2; André & Deutsch, 1984; André, 1991b, André, pers. comm. 2000). On the basis of strong geochemical similarities, the volcanic rocks of the late Caradoc – early Ashgill Madot Formation in the Fauquez area (Vanmeirhaeghe *et al.*, 2005) may have been derived from this volcano (or volcano complex) at Quenast (André, 1991b).

The Quenast microdiorite plug intrudes predominantly fine-grained, homogenous Middle to Upper Ordovician siliciclastic deposits (André, 1991b; Herbosch *et al.*, in press b). From the WNW to the ENE of the plug (outcrops Gralex 1 to 3, Quenast 4; Fig. 2) homogeneous, fine-grained, dark bluish grey to grey mudstones of the Rigenée

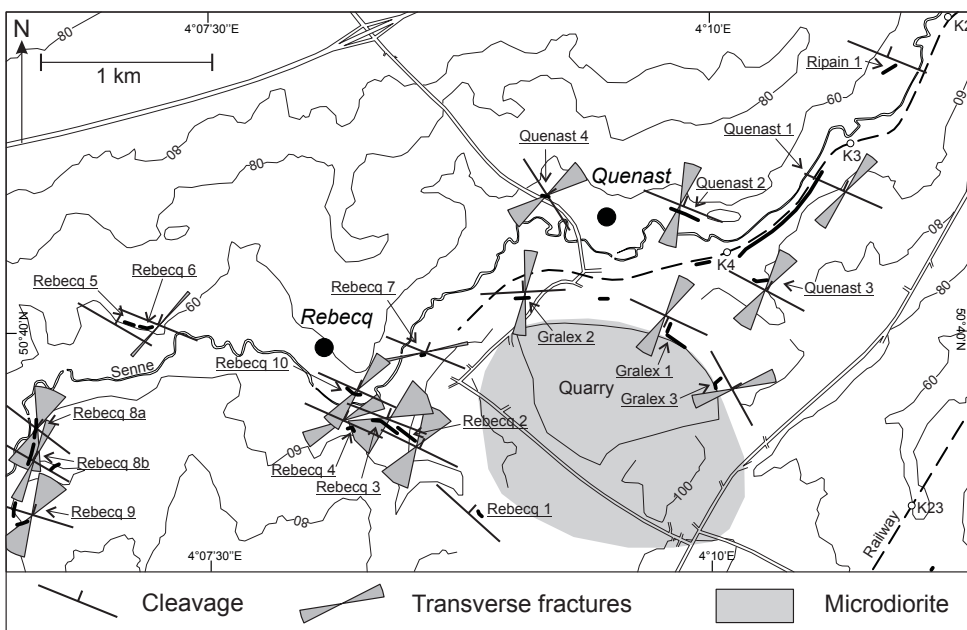


Figure 2 : Simplified topographic map of the Quenast area, showing the trend of cleavage and transverse fractures within the main outcrops. Note the change in cleavage and fracture trend around the microdioritic Quenast plug.

Formation occur (Llanvirn; cf. Lenoir, 1987). To the south and west of the plug, at Rebecq (outcrops Rebecq 1 to 4, 7, 8a, 8b and 10; Fig. 2), homogeneous, fine-grained creme-coloured mudstones of the recently defined Hospice de Rebecq Formation (Herbosch, 2005) are encountered. Further to the northwest (outcrops Rebecq 5 and 6; Fig. 2), the Bornival Formation occurs, consisting of micaceous, dark blue-grey mudstones with intercalated thin, diffuse, silty layers. To the NE of the plug, the Abbaye de Villers Formation is encountered (outcrops Quenast 2 and 3 and southern part Quenast 1; Fig. 2; cf. Lenoir, 1987), consisting of a centimetric alternation (often with diffuse limits) of bioturbated, micaceous crème-coloured to pale-grey fine sandstone and siltstone and dark blue-grey to black mudstone. Finally, further to the NE, extremely homogenous, greenish grey (S) and dark blue-grey (N) mudstones of the Lower to lower Middle Cambrian Oisquercq Formation occur (outcrop Ripain 1 and northern part of outcrop Quenast 1; Fig. 2). The limit between the Oisquercq Formation and the Lower Ordovician is formed by the Asquemont Detachment System, a recently defined pre-cleavage and pre-folding low-angle extensional detachment, visible in outcrop Quenast 1 (Debacker *et al.*, 2003, 2004a; Herbosch *et al.*, in press b).

The contact between the microdiorite and the host-rock can only be observed at the N-side of the plug, at the northern extremity of the quarry (outcrops gralex 1 and 3; Rigenée Formation). Despite the large volume of the plug, there are no observations of a significant contact-metamorphic aureole. According to Andre (1991b) this apparent absence of a contact-metamorphic aureole along the N-side of the plug may be due to later strike-slip faulting (see André & Deutsch, 1985).

3. Structural field observations

3.1. Changes in cleavage trend around the Quenast plug

On the basis of the position within the Brabant Massif (e.g. De Vos *et al.*, 1993), the distribution of the different lithostratigraphic units (e.g. Herbosch *et al.*, in press b) and the structural style within surrounding outcrop areas such as the Marcq area and the Sennette outcrop area (e.g. Sintubin, 1997; Debacker, 1999; Debacker *et al.*, 2003, 2005a; Verniers *et al.*, 2005), a NW-SE-trending,

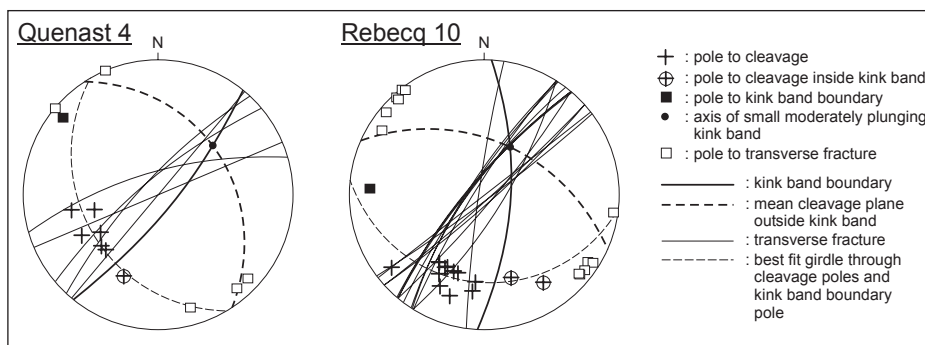


Figure 3 : Lower-hemisphere equal area projections showing cleavage, fracture and kink band data of outcrops Quenast 4 and Rebecq 10. These kink bands are referred to in the text and in Fig. 5 as set 1. Note that in both outcrops the relative orientation of the structural elements is virtually identical, and that those of outcrop Quenast 4 are rotated by ~20 to 40° clockwise with respect to those of outcrop Rebecq 10 (see also Figure 2).

Outcrop	Lithostratigraphy	Cleavage (S1)	S1 intensity	Fractures
Ripain 1	Oisquercq Fm.	n = 5; mean: 292/68N ± 003°	2	/
Quenast 1	Oisquercq-Abb. Fm	n = 31; mean: 294/63NE ± 010°	2	n = 15; mean: 038/82SE ± 009°
Quenast 2	Abbaye de Villers Fm	n = 18; mean: 292/36N ± 016°	1	n = 12; mean: 198/80NW ± 012°
Quenast 3	Abbaye de Villers Fm	n = 21; mean: 298/66NE ± 007°	2	n = 9; mean: 034/74SE ± 014°
Quenast 4	Rigenée Fm	n = 5; mean: 327/45NE ± 012°	2	n = 5; mean: 235/83NW ± 014°
Gralex 1	Rigenée Fm	n = 29; mean: 115/78SW ± 005° (pluton: 320/67NE±005° (n = 5))	4	n = 9; mean: 031/83SE ± 012°
Gralex 2	Rigenée or Bornival Fm	n = 26; mean: 267/64N ± 006°	2-3	n = 8; mean: 008/76E ± 009°
Gralex 3	Rigenée Fm	n = 21; mean: 331/59NE ± 008°	3-4	n = 4; mean: 072/89S ± 009°
Rebecq 1	Hospice de Rebecq Fm	n = 3; mean: 312/61NE ± 002°	2	/
Rebecq 2	Hospice de Rebecq Fm	n = 11; mean: 296/57NE ± 005°	2	n = 8; mean: 033/89SE ± 021°
Rebecq 3	Hospice de Rebecq Fm	n = 6; mean: 291/51N ± 003°	2	n = 6; mean: 058/88NW ± 027°
Rebecq 4	Hospice de Rebecq Fm	n = 6; mean: 294/52NE ± 007°	2	n = 4; mean: 063/81SE ± 011°
Rebecq 5	Bornival Fm	n = 5; mean: 300/53NE ± 004°	2	/
Rebecq 6	Bornival Fm	n = 11; mean: 292/55N ± 006°	2	n = 4; mean: 042/83SE ± 002°
Rebecq 7	Hospice de Rebecq Fm	n = 1; 292/55N	0-1	n = 2; mean: 258/79N ± 000°
Rebecq 8a	Hospice de Rebecq + Bornival Fm	n = 17; mean: 307/36NE ± 010°	2	n = 17; mean: 199/83W ± 023°
Rebecq 8b	Hosp. de Reb. + Huet + Fauquez Fm	n = 19; mean: 300/42NE ± 010°	2	n = 17; mean: 204/83W ± 007°
Rebecq 9	Madot Fm	n = 4; mean: 287/16N ± 014°	1-2	n = 6; mean: 211/89NW ± 021°
Rebecq 10	Hospice de Rebecq Fm	n = 13; mean: 294/57NE ± 012°	2	n = 12; mean: 219/86NW ± 012°

Table 1 : Mean cleavage and fracture orientation in the Quenast area, together with a cleavage intensity code based on a macroscopic evaluation of the cleavage (see Table 2 for significance of code).

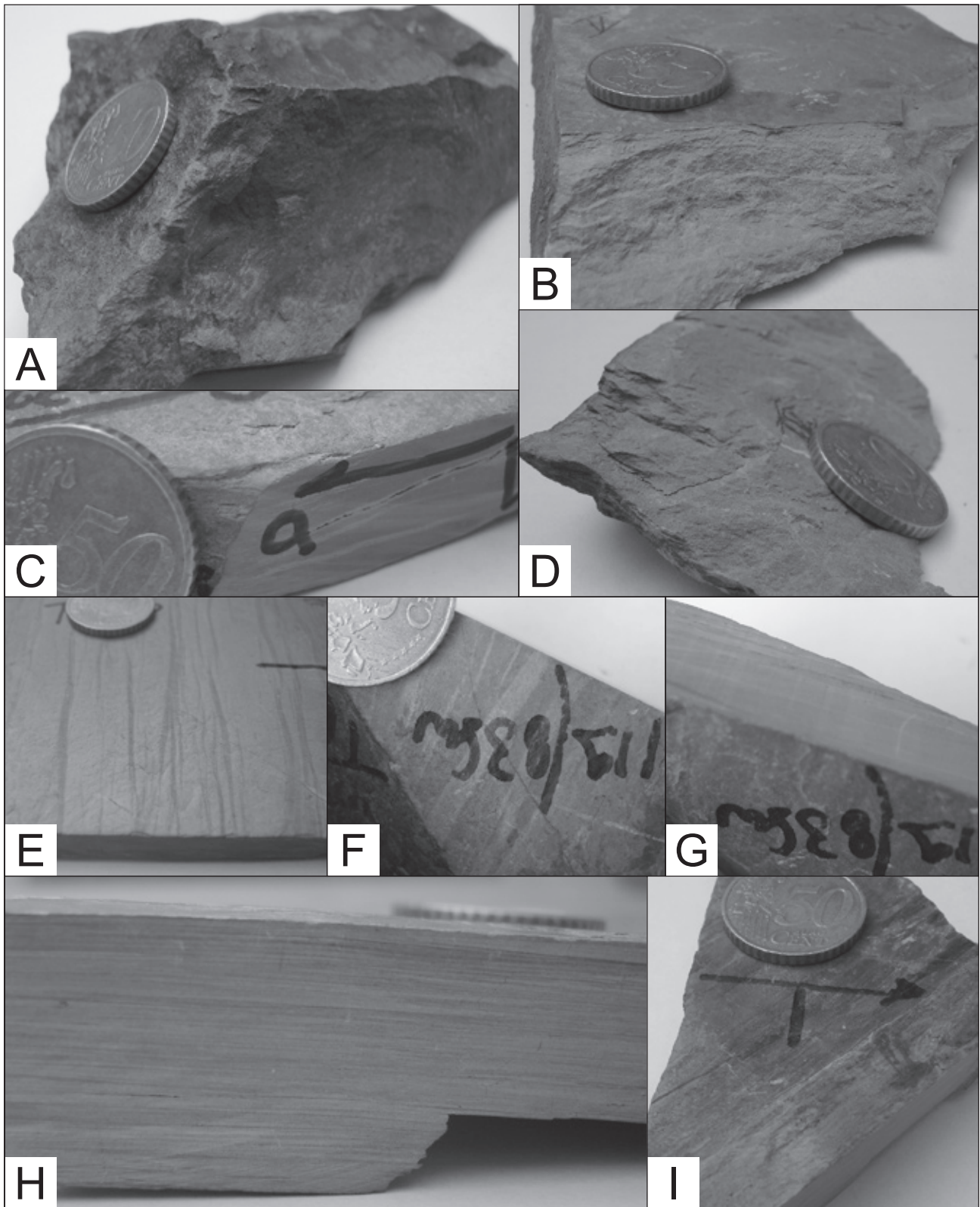


Figure 4 : Photographs of cleavage fabrics in the Quenast area (compare with Tables 1 and 2). A: Very poorly developed cleavage (code 0-1; outcrop Rebecq 7; Hospice de Rebecq Formation). B: Well developed cleavage (code 2; outcrop Rebecq 8b; Hospice de Rebecq Formation). C: Very well developed cleavage (code 3; outcrop Gralex 3; Rigenée Formation; sample TD328). D: Well developed cleavage (code 2; outcrop Rebecq 8a; Hospice de Rebecq Formation). E: Extremely well developed cleavage, with steeply plunging sinistral kink bands (code 4; set 2 kink bands; outcrop Gralex 1; Rigenée Formation; sample TD320). F: Very well to extremely well developed cleavage, with steeply plunging sinistral kink bands, viewed perpendicular to cleavage (code 3-4; set 2 kink bands; outcrop Gralex 1; Rigenée Formation; sample TD330). G: Very well to extremely well developed cleavage, with steeply plunging sinistral kink bands, viewed oblique to cleavage (code 3-4; set 2 kink bands; outcrop Gralex 1; Rigenée Formation; sample TD330). H: Extremely well developed cleavage (code 4; outcrop Gralex 3; Rigenée Formation; sample TD329). I: Extremely well developed cleavage, with moderately plunging mineral lineation on cleavage plane (code 4; outcrop Gralex 3; Rigenée Formation; sample TD329). Coin (50 eurocent) for scale.

moderately NE-dipping cleavage is expected in the study area. As shown on the map of Fig. 2, this holds true for only a part of the study area. Although the predominant cleavage orientation is indeed as expected (e.g. outcrops Rebecq 3-6, 8a, 8b, 9, 10, Ripain 1, Quenast 1-3) a marked large-scale change in cleavage trend occurs in the vicinity of the plug. In the deposits of the Rigenée Formation (outcrops Gralex 1-3) along the N-side of the plug, cleavage trend changes from NNW-SSE in the east towards E-W in the west (change of $\sim 64^\circ$), thus mimicking the northern limit of the plug (see also Table 1). Although less obvious due to the degree of exposure, a similar change occurs along the SW-side of the plug (outcrops Rebecq 1 and 2).

Outcrop Quenast 4 has a cleavage orientation that is markedly different from that in the surrounding outcrops (compare with outcrops Quenast 2 and Gralex 1) and which does not mimic the northern limit of the plug (Fig. 2). This outcrop, however, is characterised also by a pervasive brittle to brittle-ductile post-cleavage deformation, consisting of post-cleavage crush-breccias, cleavage-parallel slip surfaces and associated post-cleavage folds, which can be attributed to (seemingly reverse) faulting. When this outcrop is compared with outcrop Rebecq 10, it becomes clear that the cleavage, fractures and kink bands in outcrop Quenast 4 are all rotated by the same amount ($\sim 20\text{-}40^\circ$ clockwise) with respect to the cleavage, fractures and kink bands in outcrop Rebecq 10 (Fig. 3). Hence, the deviating orientation of the structural features in outcrop Quenast 4 is a local phenomenon, likely related to post-cleavage fault activity.

Judging from the observations in outcrops Gralex 1 to 3, the zone in which cleavage orientation mimics the plug-host rock contact extends for at least 200 m, measured perpendicular to cleavage.

3.2. Apparent variations in cleavage intensity

The largest part of the area is characterised by a poorly to well developed cleavage (codes 1 and 2 in Table 1; see also Table 2 and Fig. 4). Such a poorly to well developed

cleavage is quite comparable to that encountered in other outcrop areas (e.g. Sennette area; Debacker *et al.*, 1999, 2001, 2003, 2004b). However, if we compare the well-developed cleavage of outcrops Quenast 1 and Quenast 3 with the cleavage in the same formations in the Sennette area (Oisquercq Formation, Chevlipont Formation, Abbaye de Villers Formation), it becomes clear that, macroscopically, cleavage in outcrops Quenast 1 and 3 has a closer spacing and more regular surface, than in the same formations in the Sennette outcrop area (e.g. Debacker, 2001; Debacker *et al.*, 2003, 2004b).

Going from outcrops Quenast 1 and 3 towards the plug, a marked increase in cleavage intensity can be inferred. In outcrop Gralex 3, and to some extent also in outcrop Gralex 2, a very well developed cleavage is present, whereas in outcrop Gralex 1, also consisting of the Rigenée Formation, the cleavage is extremely well developed, with a silvery sheen and phyllitic appearance (Table 1; Figs 2 & 4). The southeasternmost part of outcrop Gralex 1 contains the northern extremity of the plug, separated from the Rigenée Formation by a steep fault zone. In the northernmost two meters, the plug shows an irregular, moderately NE-dipping foliation. This foliation is parallel to the preferred orientation of seemingly flattened feldspars, suggesting the local presence of a tectonic fabric in the plug.

In the deposits of the Hospice de Rebecq Formation in outcrop Rebecq 7, situated to the west of the plug, in the prolongation of the long axis of the plug, cleavage is almost absent (code 0 to 1), whereas to the southwest (outcrops Rebecq 2-4, 10; Hospice de Rebecq Formation) and further to the west (outcrops Rebecq 5-6; Bornival Formation; outcrops 8a, 8b; Hospice de Rebecq Formation) again a well developed cleavage is present (code 2; Table 1, Figs 2 & 4).

3.3. Changes in transverse fracture trend around the Quenast plug

Transverse fractures (or transverse joints or cross-joints), are steep fractures oriented approximately normal to any strong linear structure (e.g. Sedgwick, 1835; Turner &

Code	Term	Description
0	Very poor, almost absent	Hardly visible, very irregular, much lower fissility than bedding; yields small, very irregular, cubic fragments of strongly variable size when hammered ~pencil structure stage of Ramsay & Huber (1983)
1	Poorly developed	Clearly visible, but relatively irregular, fissility and anisotropy comparable to that of bedding; yields small, irregular, tabular fragments when hammered ~embryonic cleavage stage of Ramsay & Huber (1983)
2	Well developed	Main rock anisotropy; better fissility than bedding; much more regular cleavage surfaces than poorly developed cleavage; yields larger, more regular, relatively thin tabular to planar fragments when hammered, as compared to poorly developed cleavage ~cleavage stage of Ramsay & Huber (1983)
3	Very well developed	Main rock anisotropy; much better fissility than bedding; very regular cleavage surfaces; yields regular, thin planar fragments when hammered
4	Extremely well developed	Seemingly forming only rock anisotropy; bedding fissility completely absent; very regular cleavage surfaces with silvery, lustrous sheen, occasionally showing mineral stretching lineation; yields regular, very thin and fragile, planar fragments when hammered

Table 2 : Significance and terminology of cleavage intensity code based on a macroscopic evaluation of the cleavage, as used in Table 1.

Outcrop/sample	S1 outside	S1 inside	KBB	Kink axis	ϕ	ϕ_k	α	β	Vol. change	Kink band type
Quenast 4	327/45NE	293/55NE	039/80SE	51/052	70	83	70	83	+5.6%	Sinistral, contractional
Rebecq 10	294/57NE	236/67N	003/74E	50/023	64	65	64	65	+0.8%	Sinistral, contractional
Rebecq 10	294/57NE	252/54N	003/74E	50/023	64	83	64	83	+10.4%	Sinistral, contractional
Gralex 1, TD320	120/86SE	105/88S	211/81W	80/274	90	75	90	105	-3.4%	Sinistral, dilational
Gralex 1, TD320	120/87S	109/86S	211/81W	80/274	89	79	89	101	-1.8%	Sinistral, dilational
Gralex 1, TD320	120/86SE	105/88S	210/86W	84/253	90	75	90	105	-3.4%	Sinistral, dilational
Gralex 1, TD320	120/87S	109/86S	210/86W	84/253	90	79	90	101	-1.8%	Sinistral, dilational
Gralex 1, TD320	120/86SE	105/88S	030/88SE	86/181	90	75	90	105	-3.4%	Sinistral, dilational
Gralex 1, TD320	120/87S	109/86S	030/88SE	86/181	90	79	90	101	-1.8%	Sinistral, dilational
Gralex 1, TD330	121/83S	112/83S	029/88SE	83/193	88	83	88	97	-0.7%	Sinistral, dilational
Gralex 1	110/81S	305/84NE	141/35SW	28/294	52	62	52	62	+12.0%	Top-to-S, contractional
Gralex 1	120/77S	295/66NE	134/23SW	07/298	55	88	55	88	+22%	Top-to-S, contractional

Table 3: Kink band data and geometrical analysis of three types of kink bands encountered in the Quenast area. S1: cleavage; KBB: kink band boundary; ϕ : angle between regional cleavage and KBB (Srivastava et al., 1998); ϕ_k : angle between cleavage inside kink band and KBB (Srivastava et al., 1998); α : angle between KBB and regional cleavage, measured outwards toward regional cleavage (Anderson, 1964; cf. Ramsay & Huber, 1987); β : angle between cleavage inside kink band and KBB, measured in same sense as α (Anderson, 1964; cf. Ramsay & Huber, 1987); Vol. change: volume change inside kink band, due to kink band development, given by formula $\sin \beta / \sin \alpha - 1$ (Anderson, 1964; cf. Ramsay & Huber, 1987). See also Fig. 5 for geological significance of different angles and values.

Weiss, 1963; cf. Dennis, 1967). In the Brabant Massif, the transverse fractures, usually without infill, are commonly the most obvious and continuous of all (barren) fractures present and occur at high angles to the fold hinge lines and the cleavage/bedding intersection (e.g. Debacker, 2001; Debacker *et al.*, 2001, 2004b).

As can be seen on Fig. 2 and in Table 1, the transverse fractures occur throughout the Quenast area and show a marked change in trend around the plug, very similar to the trend change shown by cleavage. The fractures are

always at high angles to the cleavage (hence the similar change in trend), but only along the N- and NE-side of the plug are the fractures subperpendicular to the plug (e.g. fractures are not perpendicular to the plug in outcrops Rebecq 2-4, 10). In contrast to the cleavage, there appears to be no obvious change in fracture intensity or spacing across the area. This, in combination with the relative orientation of the fractures with respect to the plug, implies that the measured fractures are indeed true transverse fractures, quite different from fractures related

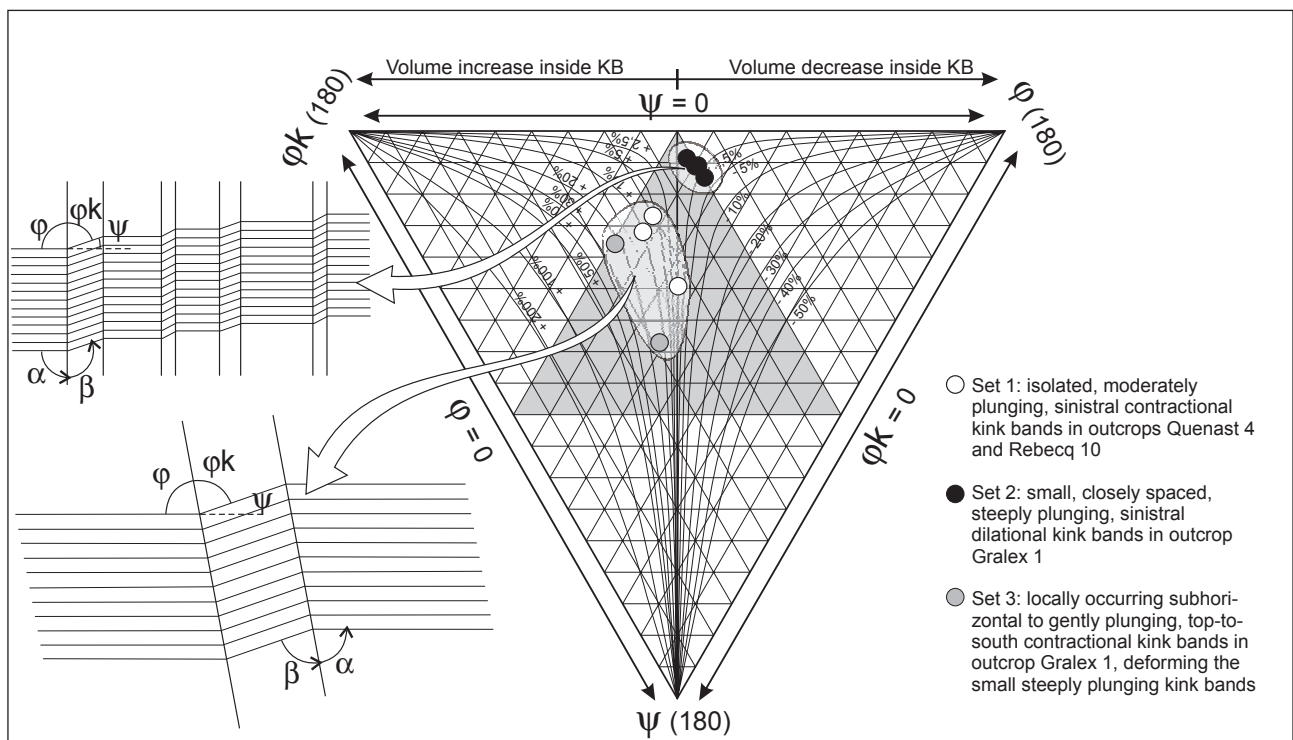


Figure 5: The internal geometry of the three types of kink bands recognised in the Quenast area (sets 1 to 3), visualised on a kink band triangle of Srivastava et al. (1998), on which we added lines of volume change given by the formula $\sin \beta / \sin \alpha - 1$ of Anderson (1964; see also Table 3). Note the two different fields occupied by kink bands of set 2 on the one hand (dilational kink bands) and kink bands of sets 1 and 3 on the other hand (contractional kink bands). For clarity, a schematic representation is given of both groups of kink bands, with indication of the angles α , β (Anderson, 1964), ϕ , ϕ_k and ψ . See also Figs 3 and 6.

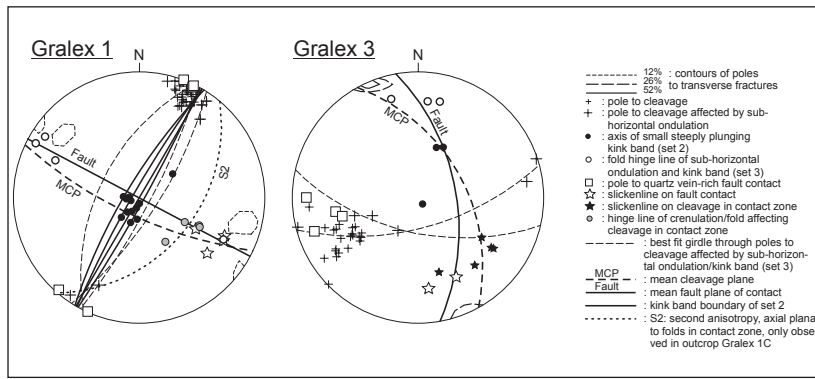


Figure 6: Lower-hemisphere equal area projections showing cleavage, fracture, kink band and fault data of outcrops Gralex 1 and Gralex 3. Note that in both outcrops kink bands of set 2 and set 3, occur, the latter deforming the former. Within the fault zone in outcrop Gralex 1, however, seemingly a fourth kind of small-scale, post-cleavage fold occurs, having moderately E-plunging axes and being locally accompanied by a spaced, moderately SE-dipping second cleavage (S2). Possibly these folds, and their associated foliation, correspond to the kink bands of set 2, that have rotated towards a less steep orientation as a result of later fault movement.

to magma emplacement. In the latter case, fractures would show a radial pattern around the plug (subperpendicular to the plug along all sides), and a marked change in intensity and spacing with distance from the plug.

3.4. Post-cleavage folds, kink bands

As outlined above, in outcrops Quenast 4 and Rebecq 10 very locally kink bands are observed (Fig. 3). In both outcrops these kink bands, referred to as set 1, have an identical geometry, with a sinistral asymmetry, kink band widths of 1 to 3 cm, steep to subvertical kink band boundaries and a moderately NE-plunging kink axis. These kink bands are of a contractional type, with an inferred volume increase inside the kink band of up to ~10% (Table 3, Fig. 5). As such, these kink bands reflect a subhorizontal shortening direction at low angles to cleavage, oriented slightly clockwise with respect to cleavage trend. Assuming that the orientation of the transverse fractures, cleavage and kink bands in outcrop Quenast 4 was originally similar to that in outcrop Rebecq 10 (see above and Fig. 3), but was rotated by later faulting, the kink bands in both outcrops would reflect a similar subhorizontal, (N)NW-(S)SE-directed shortening direction.

The most apparent kink bands of the Quenast area, however, are found in the very well to extremely well

cleaved rocks of the Rigenée Formation in outcrop Gralex 1 and less commonly in outcrop Gralex 3. These kink bands, referred to as set 2, are markedly different from the large isolated kink bands of set 1 described above. The kink bands in outcrops Gralex 1 and 3 have kink band widths of only 0.5 to 3 mm, and occur very frequently, with a spacing of only 1 mm to 2 cm (Figs 4 & 5). Because of the homogeneity of the deposits, the close spacing of the kink bands and the small kink band dimensions, their internal geometry is difficult to measure. The detailed internal geometry shown in Table 3 and described below is based on oriented samples and outcrop observations from outcrop Gralex 1. The kink bands have a sinistral geometry and steeply plunging kink axes, oriented subparallel to the cleavage dip direction. The subvertical kink band boundaries are oriented perpendicular to cleavage (α or $\phi \sim 90^\circ$; see Table 3; Figs 5 & 6). Judging from the literature, such a kink band boundary orientation is quite exceptional, and resembles that of pelitic strain bands of Dewey (1965). Although having a slightly anastomosing nature, the kink band orientation is quite constant. An analysis of the internal geometry indicates that these kink bands have a dilational nature, with an inferred volume decrease inside the kink band of up to ~4% (Table 3, Fig. 5). Judging from the internal geometry, these kink bands reflect a subhorizontal shortening direction at moderate to high angles to cleavage, oriented

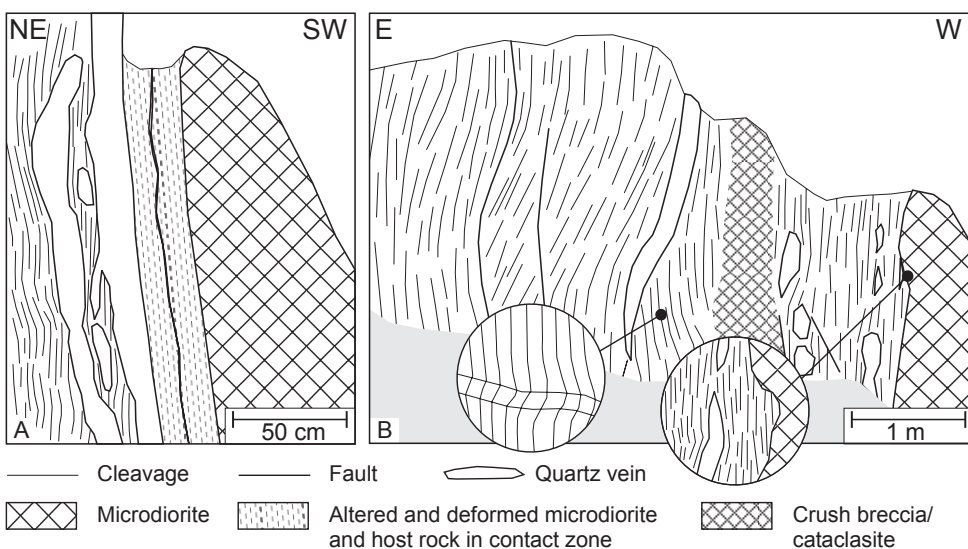


Figure 7: Line-drawing of the contact zone between the fine-grained siliclastic rocks of the Rigenée Formation (N, NE, E) and the microdioritic plug (S, SW, W) in outcrops Gralex 1 (A) and Gralex 3 (B). The circular insets in (B) show a subhorizontal to gently inclined, subhorizontal to gently plunging contractional kink band (left; see also Fig. 6) and a(n) original non-tectonic contact between the Rigenée Formation and the microdiorite, the former without macroscopic evidence of contact metamorphism (right). Note the deformed quartz veins in the contact zone.

- Cleavage
- Fault
- Quartz vein
- Microdiorite
- Altered and deformed microdiorite and host rock in contact zone
- Crush breccia/cataclasite

clockwise with respect to cleavage trend (e.g. Cobbold *et al.*, 1971).

In both outcrops (outcrops Gralex 1 and 3) the kink bands of set 2 are deformed by gentle, subhorizontal to gently plunging, post-cleavage folds, often only visible as gentle undulations in cleavage dip. Locally these structures become more angular and become contractional kink bands with gently SW-dipping axial surfaces and a top-to-the-south asymmetry (Figs 5, 6 & 7B, Table 3). The geometry of these folds and kink bands, referred to as set 3, reflects development under the influence of a steeply S-plunging shortening direction. Although in outcrop Gralex 3 these structures occur in the vicinity of a supposedly important fault (e.g. Fig. 7B; André & Deutsch, 1985) and might be interpreted as directly being related to the fault activity, this is apparently contradicted by their occurrence in the northern part of outcrop Gralex 1, well away from the fault contact.

3.5. The fault zone along the NE-side of the plug

As already pointed out by André & Deutsch (1985), in outcrop Gralex 3 and the eastern parts of outcrop Gralex 1 a fault zone occurs at the contact between the Rigenée Formation and the microdiorite. In both outcrops, the fault zone between the Rigenée Formation and the plug contains numerous quartz veins, oriented parallel to the contact (Fig. 7). Whereas in outcrop Gralex 1 the quartz vein-bearing fault zone locally reaches a thickness of more than 10 metres (almost entirely vein quartz), the quartz vein-bearing fault zone only has a thickness of several decimetres in outcrop Gralex 3. Although André & Deutsch (1985) consider these contacts in both outcrops as belonging to two different faults, we managed to trace the same fault zone in between both outcrops. Hence, like the cleavage and the transverse fractures, also the quartz vein-bearing fault zone shows a marked change in trend between outcrops Gralex 1 and Gralex 3.

A gently to moderately SSE-plunging lineation/slickenline on cleavage planes (e.g. sample TD329; see below) and quartz vein surfaces in outcrop Gralex 3 suggests an oblique, dextral sense of movement (Fig. 6). The nature of the quartz veins (incorporated in crush breccias, protocataclasites and gently folded) in the contact zone indicates additional deformation after quartz vein development (Fig. 7B). This fault-related, post-cleavage deformation is associated with a change in orientation of the cleavage and of the axial surfaces/kink band boundaries of the subhorizontal to gently plunging open folds and kink bands (set 3): in zones of moderately E-dipping cleavage, the kink band boundaries dip moderately towards the west, whereas in zones of steeply E-dipping cleavage, the kink band boundaries dip gently towards the west (e.g. Fig. 7B). As such, at least part of the deformation associated with the fault zone forming the NE-limit of the Quenast plug took place during or after the development of the subhorizontal folds and kink bands (set 3), of which the orientation suggests development under the influence of a subvertical to steeply plunging shortening.

Also outcrop Gralex 1 contains moderately to gently SE-plunging slickenlines on quartz vein surfaces (Fig. 6). Although one of these suggests a dextral movement, comparable with the observations in outcrop Gralex 3, the cleavage planes close to the fault zone locally contain small, open crenulations, with moderately SE-plunging axes that are subparallel to the slickenlines on the quartz vein surfaces (Fig. 6). As such, care should be taken when interpreting these apparent slickenlines. The crenulations are accompanied locally by a spaced fabric (S2 in Fig. 6), representing the crenulation axial surface. Possibly, these crenulations and the associated spaced fabric correspond to the steeply plunging kink bands of set 2. Indeed, in this part of the outcrop, kink bands of set 2 were not recognised as such, and it is not unlikely that these locally occurring crenulations represent smaller, more irregular variants of the kink bands of set 2, that have rotated to a less steep orientation (rotation of $\sim 40^\circ$ around pole to fault contact) close to the fault zone. Locally in outcrop Gralex 1, close to the fault zone, also a steep slickenline/lineation is present on cleavage surfaces (e.g. sample TD331; see below).

4. Fabric analysis

In order to check the macroscopic evaluation of the cleavage intensity, pole figure goniometry was performed on selected oriented samples of different formations within the Quenast area. This was done by means of an X-ray pole figure goniometer using Fe-filtered Co-radiation (40kV x 30 mA). Complete normalised pole figures were obtained by combining incomplete pole figure measurements, performed in transmission mode, on two mutually perpendicular sections of the sample, both perpendicular to the main foliation (cleavage). A more extensive description of the procedure can be found in Sintubin *et al.* (1995). For each sample, both mica (001) ($d = 1.0$ nm) and chlorite (002) ($d = 0.7$ nm) orientation distributions were measured. The phyllosilicate preferred orientations are evidenced using contoured orientation distributions (lower-hemisphere equal-area projections). Contours represent “multiples of a random distribution” (mrd). The interpretation of the pole figures is based, on the one hand, on the pole figure patterns (Sintubin 1994, 1998), taking into account the symmetry of the orientation distribution and its angular relationship with distinct fabric elements (bedding, cleavage,...), and, on the other hand, on the degree of preferred orientation (see Fig. 8).

Pole figure goniometry was performed on two samples of the Asquempont Member (Oisquercq Formation) from outcrop Quenast 1 (Fig. 8). In both samples the degree of preferred orientation is slightly higher for mica than for chlorite. In sample TD335, both mica and chlorite are centred around the cleavage pole and have a moderate degree of preferred orientation, with a slight orthorhombic symmetry. It may either be interpreted as a weakly developed intersection pole figure pattern with an intersection lineation parallel to the dip direction of the cleavage, or, taking into account the moderate degree of

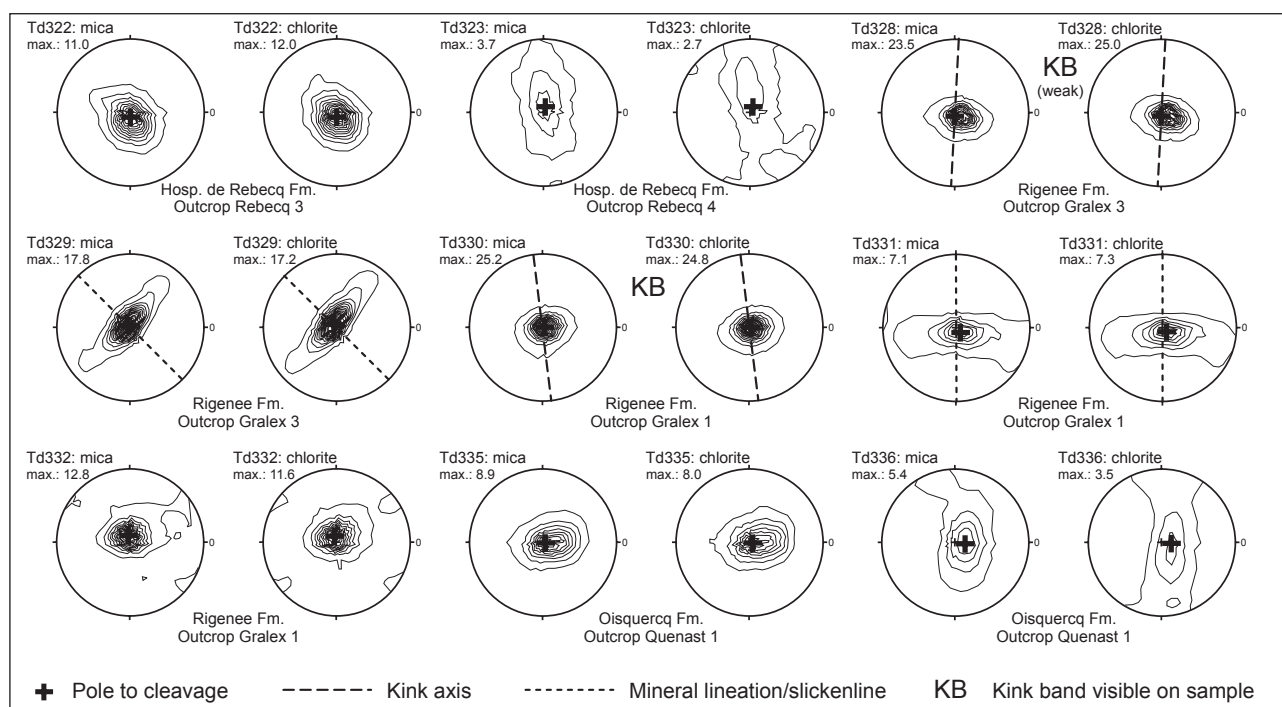


Figure 8 : Phyllosilicate X-ray pole figures of white mica (d001; left) and chlorite (d002; right) from the Hospice de Rebecq Formation (samples TD322, TD323), the Rigenée Formation (samples TD328 to TD332) and the Oisquercq Formation (samples TD335, TD336) around the Quenast plug, together with the projected positions of the cleavage poles. Where possible, the orientation of specific features such as kink band axes and mineral lineations is added, as well as the presence of kink bands on the analysed sample (KB). For each sample, for both white mica and chlorite, the maximum degree of preferred orientation, expressed in multiples of a random distribution (mrd) is indicated (max.:). Contours are per unit of 1 mrd (1, 2, 3,...), except for samples TD328, TD329 and TD330 where, due to the high degree of preferred orientation, for clarity, contours are per 2 mrd (1, 3, 5,...). Note the very high degree of preferred orientation observed within the Rigenée Formation in outcrops Gralex 1 and Gralex 3.

preferred orientation and the poorly developed orthorhombic symmetry as a flattening fabric resulting from cleavage development. In contrast, sample TD336, with a weak (chlorite) to moderate (mica) degree of preferred orientation, shows a well-developed orthorhombic pole figure pattern for mica and a girdle symmetry for chlorite, both centred around the cleavage pole. Hence, sample TD336 likely reflects an intersection fabric, with a subhorizontal intersection lineation. This intersection lineation is probably the cleavage/bedding intersection. Indeed, across the Quenast area, both the syn-cleavage folds and the cleavage/bedding intersection are subhorizontal to gently plunging.

Two samples from two outcrops at Rebecq, to the SW of the Quenast plug, have a relatively weak (TD323) to high (TD322) degree of preferred orientation (Fig. 8). In the latter case, a pure flattening fabric becomes apparent, in the former case an orthorhombic to girdle pole figure pattern. The girdle pattern of sample TD323, which is better developed for chlorite than for mica, suggests a subhorizontal intersection lineation, probably representing the cleavage/bedding intersection.

Samples from the Rigenée Formation from outcrops Gralex 1 and Gralex 3, along the NE-side of the Quenast plug, were taken well away from the fault zone, in order to avoid any possible artefacts related to fault activity (the closest samples, TD328 and TD329, were taken at 10 m E of the fault contact). With one exception (TD331;

moderate), samples from the Rigenée Formation from outcrops Gralex 1 and Gralex 3 have a high (TD332) to extremely high (TD328, TD329, TD330) degree of preferred orientation, which is similar for chlorite and white mica (Fig. 8). The pole figure patterns, centred around the cleavage pole, generally have an axially symmetrical (TD328, TD330, TD332) to orthorhombic (girdle; TD329, TD331) pole figure pattern. An analysis of the orientation of the long axes of the axially symmetrical pole figure patterns shows that these are commonly oriented at right angles to the axes of the steeply plunging small-scale kink bands of set 2 (e.g. TD328, TD330). These samples reflect a predominant flattening fabric (similar to sample TD332), in which the slight asymmetry is compatible with the internal geometry of the steeply plunging kink bands and hence might indeed be due to the pervasive small-scale kinking. The orthorhombic to girdle pole figure pattern of samples TD329 and TD331 cannot be explained by means of kink bands, as the ratios are much too high for the $\sim 15^\circ$ change in cleavage trend due to kink band development. In addition, the high ratio of the orthorhombic pole figure pattern of sample TD329 (outcrop Gralex 3) suggests a pronounced differential stretching in the cleavage plane. Indeed, the short axis of the pole figure pattern of sample TD329 is parallel to a pronounced, moderately SE-plunging mineral lineation that is at high angles to nearby kink axes. Also the girdle pattern of sample TD331 (outcrop Gralex 1) can be

explained in a similar way. This sample does not show macroscopically recognisable kink bands, but does have a weakly developed lineation/slickenline that is oriented subparallel to the axes of steeply plunging kink bands in the same outcrop.

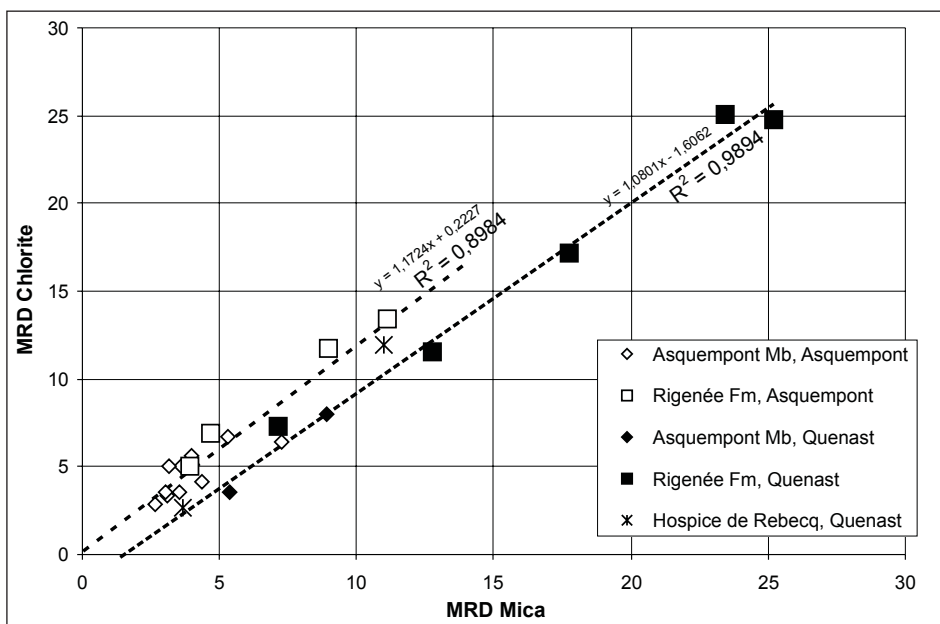
5. Interpretation of fabric analysis

Figure 9 shows a graph of the degree of preferred orientation of chlorite and white mica of samples of the Asquempont Member and the Rigenée Formation from both the Asquempont outcrop area (Sennette valley) and the Quenast outcrop area (Senne valley). On this graph, two apparent differences can be observed between the lithostratigraphic units in the Asquempont area and the same units in the Quenast area. Firstly, most samples of the Rigenée Formation at Quenast have a much higher degree of preferred phyllosilicate orientation than the samples of the Rigenée Formation at Asquempont. For the Asquempont Member, the degree of preferred orientation for both mica and chlorite are similar to only slightly higher at Quenast than at Asquempont. However, at Asquempont chlorite consistently has a preferred orientation subparallel to bedding (Debacker *et al.*, 2004c), whereas at Quenast, chlorite has a preferred orientation parallel to cleavage. Secondly, for both units the amount of preferred orientation of white mica with respect to that of chlorite is different at Quenast and at Asquempont. Whereas at Asquempont the degree of preferred orientation of chlorite is higher than that of white mica, at Quenast the degree of preferred orientation of chlorite is similar to slightly lower than the degree of preferred orientation of white mica. On Fig. 9, this difference is reflected by a rightward shift of the samples of Quenast with respect to those at Asquempont. Hence, it appears that the increase in cleavage intensity is reflected better by the increase of degree of preferred orientation of white mica than by that of chlorite.

The high to very high degree of cleavage-parallel phyllosilicate preferred orientation in samples of the Rigenée Formation at Quenast points to the presence of a high-strain zone. The presence of a high-strain zone is fully compatible with the phyllitic appearance of the cleavage. Despite the rather similar degree of phyllosilicate preferred orientation, also the change from a predominantly bedding-parallel chlorite fabric in the samples of the Asquempont Member at Asquempont to a predominantly cleavage-parallel chlorite fabric in the samples of the Asquempont Member at Quenast suggests a more pronounced cleavage fabric and a more intense (tectonic) finite strain at Quenast. Also this is compatible with the macroscopic evaluation of the cleavage intensity (see above). Judging from the X-ray pole figure goniometry results and the macroscopic cleavage evaluation (Figs 8, 9 & Table 1), this high-strain zone runs along the NE-side of the plug, with the zone of maximum strain intensity (“centre” of high-strain zone) occurring in outcrops Gralex 1 and 3. Apparently, strain gradually decreases towards the NE.

As indicated by the X-ray pole figure goniometry results from within the high-strain zone along the NE-side of the plug, in the cleavage plane locally differential stretching (TD329) occurs. In addition, locally much less deformed rocks (TD331) are present in between more strongly deformed rocks (TD330, TD332). These observations suggest strain partitioning and strain localisation within the high-strain zone.

The March model (March, 1932), relating the phyllosilicate orientation distributions to strain, assuming passive rotation of platy fabric elements (cf. Oertel, 1983), can be used to estimate the amount of cleavage-related shortening. Based on the March model, the calculated shortening in the high-strain zone at the NE-side of the plug has a mean value of ~60%, with a maximum of ~66% (samples TD328 and TD330) and a minimum of ~48% (sample TD331; lower values due to differential stretching



within cleavage plane; see Fig. 8 and higher). Outside this high-strain zone, calculated shortening values are significantly lower, ranging between ~36 and ~55%, with a mean value of ~45%. The latter values may be considered as a regional average for the calculated cleavage-related shortening in the fine-grained siliciclastic deposits in the Quenast area.

Although tectonic high-strain zones moulding intrusive bodies are common (e.g. Walcott & Craw, 1993; Mamtani & Greiling, 2005; Passchier *et al.*, 2007), the question may be put forward whether the strain within the high-strain zone is entirely due to tectonic shortening. As suggested by André (pers. comm., 2007), the high heat flow from the cooling plug might have caused significant dehydration of the wall rock, eventually resulting in a flattening fabric subparallel to the plug. If this were to be true, the inferred tectonic strains within the high-strain zone may be overrated. Although we cannot rule out that this process actually occurred, its contribution to total strain is likely to be minor for the following reasons. a) Not only the Rigenée Formation, but also the Asquempont Member, situated well away from the contact (outcrop Quenast 1), shows higher strains than in other areas; b) Over a distance of up to 100 m from the plug, the distribution of pockets of higher and lower strain within the high-strain zone in outcrops Gralex 1 and 3 does not show any relationship with distance to the plug, something which is difficult to reconcile with magmatic heat-driven thermal dehydration of very low permeability shale (the Rigenée Formation); c) At the NE-side of the Quenast plug, there is very little evidence of contact metamorphism (André, 1991b). As argued by André (1991b), faults and shear zones within the high-strain zone may have displaced the metamorphic aureole with respect to the plug. An alternative or complementary explanation, however, is that the shale of the Rigenée Formation effectively acted as thermal barrier, resulting in only a very thin metamorphic aureole. The latter idea is compatible with the presence in outcrop Gralex 3 of a thin wedge of wall rock having an

irregular, consolidated contact with the plug, without macroscopically recognisable traces of contact metamorphism (see Fig. 7B). In summary, we feel that the inferred values from the high-strain zone can indeed be regarded as reflecting a tectonic cleavage-related shortening.

6. Discussion

6.1. Contractional deformation and relative timing of the Quenast plug emplacement

The structural observations, such as the change in transverse fracture orientation, and the change in cleavage orientation and cleavage intensity around the plug, rule out a post-kinematic emplacement, and indicate that the plug behaved as a competent body during tectonic deformation. This is further outlined below.

Fig. 10 shows the inferred cleavage trajectories across the study area. As the cleavage plane is commonly regarded as representing the XY-plane of the finite strain ellipsoid (e.g. Sorby, 1853; Siddans, 1972; Ramsay & Huber, 1983), the change in cleavage orientation around the plug reflects a large-scale bending of the XY-plane of the finite strain ellipsoid. This bending is caused by the compression of fine-grained, incompetent rocks against the magmatic body, which acted as a competent body during deformation, quite comparable to clasts in a deformed conglomerate (e.g. see Fig. 7.1. of Ramsay & Huber, 1983 and Figs 1 and 6 of Treagus & Treagus, 2002). The fact that it behaved as a competent body implies that the magmatic body had sufficiently cooled already (cf. Czeck *et al.*, 2006). Hence, the Quenast plug can be regarded as having acted as a mega-porphyroclast during the Brabantian Orogeny. This idea is further supported by the ellipsoidal cross-section of the plug, with a long axis subparallel to the cleavage trajectories and a short axis subperpendicular to the cleavage

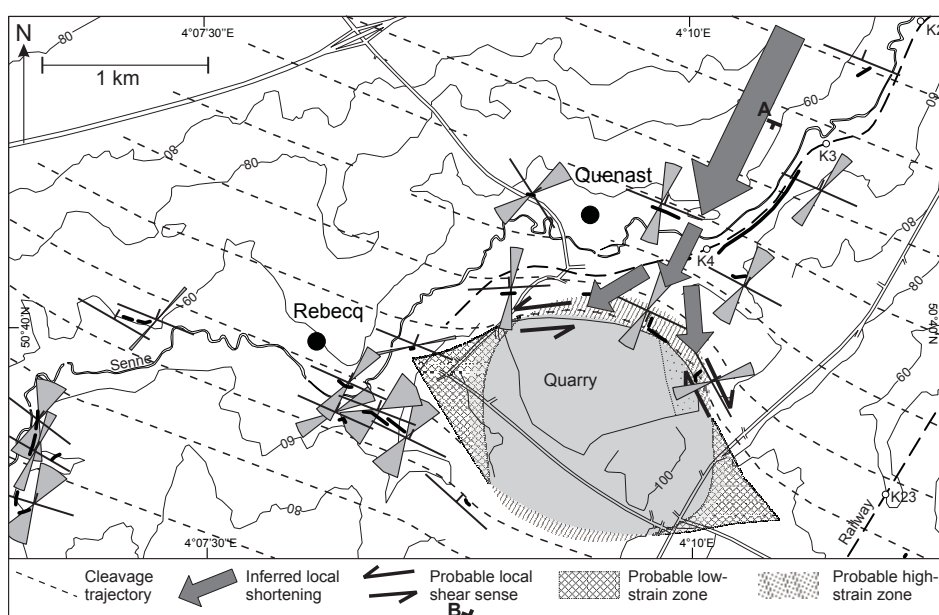


Figure 10 : Simplified topographic map of figure 2, with added inferred cleavage trajectories, inferred shortening direction, inferred and observed local shear sense, and inferred low- and high-strain zones around the Quenast plug. Also shown is an area of intense mineralisation in the NE-side of the quarry (dotted area; Vergari, pers. comm. 2000), possibly related to and extending towards the inferred low-strain zone at the SE-side of the plug. Note that the extent of the high- and low-strain zones is unknown. A-B: section line of section in Fig. 11.

trajectories, seemingly suggestive of some degree of shortening.

The shape of the cleavage trajectories reflects a NE-SW to N-S-directed shortening. Taking into account such a shortening direction acting on incompetent materials surrounding a large competent body with an ellipsoidal cross-section, several structural features are expected to develop. On the basis of the relative orientation of the host rock-plug contact with respect to shortening, three main zones can be distinguished: a frontal part (NE-side of the plug; e.g. outcrop Gralex 1), the lateral parts (NW- and SE-sides of the plug), and the intermediate parts (NNW-side and ENE-side; e.g. outcrop Gralex 3).

At the NE-side of the plug, where shortening is perpendicular to the plug, shortening is most intense and will essentially take place in the form of pure shear. In the incompetent host rocks, this intense shortening gives rise to a high-strain zone, characterised by an extremely well-developed cleavage (code 4). Within this high-strain zone, the pure shear dominated shortening may result in a vertical and lateral escape of material. The subvertical differential stretching suggested by the X-ray pole figures of sample TD331 is compatible with a vertical escape of material. The small-scale steeply plunging dilational kink bands of set 2, reflecting a shortening at moderate to high angles to cleavage, are compatible with a lateral escape of material. Also the dextral slickenlines within the fault zone are compatible with a lateral escape of material. As a result of the intense pure-shear-dominated deformation at the frontal part of the plug, a tectonic fabric may also form in the northeasternmost part of the plug itself, as observed in outcrop Gralex 1.

In contrast to the expected and observed high-strain zone at the frontal, NE-side of the plug, the lateral parts of the plug (the NW and SE-sides) will partly shield the adjacent incompetent rocks from deformation and give rise to a strain shadow. In these parts, cleavage is very poorly developed, as observed in outcrop Rebecq 7 (code 0-1), and might even be absent locally. Syntectonic fluid flow will be focussed towards these strain shadows, which extend inside the plug, and may give rise to a certain amount of mineralisation. In the case of syntectonic magma emplacement and syntectonic hydrothermal alteration, possible new intrusions would preferably form at these low-strain localities, and also hydrothermal fluids would be directed towards these low-strain localities (cf. Passchier *et al.*, 2007).

In the intermediate parts, shortening is oblique to the host rock-plug contact. This oblique shortening results in a lateral shear component in addition to the much less important shear related to the lateral escape of material at the frontal part of the plug. This shear should have a dextral sense of movement at the ENE-side (outcrop Gralex 3) and a sinistral sense at the NW-side (in the vicinity of outcrop Gralex 2). Part of this shearing will be taken up by the incompetent rocks. The oblique cleavage-parallel lineations, the oblique differential stretching suggested by the X-ray pole figures of sample TD329, and the small-scale steeply plunging dilational kink bands of

set 2, can all be attributed, at least partly, to this dextral shear. However, because of the large competence contrast between the plug and the surrounding incompetent host rock, a detachment is expected at the host rock-plug contact. As such, a fault or shear zone with a pronounced lateral component is expected to develop at the host rock-plug contact. Likely, this is reflected by the quartz vein-rich contact zone encountered in and between outcrops Gralex 1 and Gralex 3, in which dextral slickenlines have been observed (Figs 6 & 7). To the west of outcrop Gralex 1, a similar detachment is expected with a sinistral sense of movement (not observed).

The overview above clearly demonstrates that the Quenast plug behaved as a competent body during the Brabantian deformation event. This competence indicates that the magma had sufficiently cooled, and therefore we suggest a pre-kinematic emplacement age, this being compatible with Corin (1965) and with the radiometric cooling age of André & Deutsch (1984). Although, given the vast literature on synkinematic pluton emplacement (e.g. Davis & Henderson, 1999; Mamtani & Greiling, 2005; Romeo *et al.*, 2006; Passchier *et al.*, 2007; Cecys & Benn, 2007; Czeck *et al.*, 2006), it might be tempting to consider a synkinematic emplacement, there are several arguments against this. 1) As pointed out above, during synkinematic emplacement, synkinematic hydrothermal fluids, responsible for hydrothermal alteration (dated in Quenast at 438 ± 28 Ma, André & Deutsch, 1986; cf. André, 1983), would be directed towards the low-strain zones (NW and SE-parts). On the contrary, at Quenast these fluids resulted in several concentric hydrothermal alteration zones, which do not show any relationship with the low- and high-strain zones (cf. André & Deutsch, 1986). 2) A synkinematic diapiric rise of the magma, with subsequent ballooning, seemingly complies with the ellipsoidal shape at the surface and with the concentric alteration pattern and is capable of producing considerable strain in the host-rocks (Brown & McClelland, 2000). However, such an emplacement mechanism is very difficult to reconcile with the idea of a shallow volcano neck (Brown & McClelland, 2000) and would result in a tremendous amount of extension radiating all around the plug, something which is not observed. 3) Irrespective of the emplacement mechanism, synkinematic magmatic bodies commonly have geometries that reflect the kinematics of the tectonic deformation (e.g. Czeck *et al.*, 2006; Passchier *et al.*, 2007). Within the Quenast area, having experienced a NNE-SSW- to NE-SW-directed shortening, without important lateral movements (cf. Debacker, 2001), synkinematic emplacement is expected to result in a) a more elongate and more irregular ~NW-SE-trending body (growing in ~NW-SE-direction, along a developing anisotropy with possible new intrusions forming in newly generated low-strain zones), or b) an extremely elongate ~NE-SW-trending body (~NE-SW-trending dyke).

In order to further check and constrain the pre-kinematic emplacement age, the nature and importance of the pre- and post-kinematic deformation features (e.g.

normal faults) have to be assessed, as well as the exact relationship of the plug with the surrounding host rocks. These assessments provide valuable information for the deformation geometry and basin evolutionary history of the Brabant Massif.

6.2. The Nieuwpoort-Asquempont Fault Zone

Given the scenario outlined above, the fault forming the northern limit of the plug may be of local importance, without showing a large displacement. This contrasts with the opinion of André & Deutsch (1985) and André (1991b) who considered the contact in outcrops Gralex 1 and Gralex 3 as two separate zones with breccias and mylonites, responsible for a lateral displacement of the metamorphic aureole relative to the plug. However, several observations indicate that a large lateral displacement along this fault is very unlikely. Firstly, although a large-displacement fault is expected to have a considerable influence on the stratigraphic distribution, the northern part of the plug and the fault are both situated amid rocks of the Rigenée Formation (e.g. Herbosch *et al.*, in press b). Secondly, as demonstrated in this paper, all around the plug the trend of both the cleavage and the transverse fractures shows a systematic change that can be related to the geometry of the plug (Figs 2 & 10). This systematic pattern of cleavage and fracture orientations argues against the presence of an important lateral syn- or post-cleavage fault. Thirdly, in outcrop Gralex 3 a thin wedge of fine-grained siliciclastic rocks occurs in between the plug and the tectonic contact (see Fig. 7B). These sedimentary rocks of the Rigenée Formation have an irregular, consolidated contact with the plug. The latter contact shows no evidence of tectonic displacement, nor does it show macroscopically recognisable traces of contact metamorphism. This implies that there is no need for a large fault displacing a metamorphic aureole.

As such, most observations favour a local importance of this fault, which, as outlined above, is compatible with development during contraction. Several features, however, such as brecciated and folded quartz veins, point to fault reactivation. At least part of this younger fault activity took place with a different sense of movement. The change in orientation in the vicinity of the fault of the subhorizontal to gently plunging, gentle post-cleavage folds (set 3), reflecting a steeply plunging to vertical shortening, points to fault movement during or after subvertical shortening, post-dating the contractional deformation. Also steeply plunging slickenlines on cleavage planes may be related to this younger fault activity.

Following Legrand (1968), several authors mention the presence of a wide, steep fault zone between Nieuwpoort and Asquempont (Oudenaarde-Bierghes fault zone of Legrand, 1968 and André & Deutsch, 1985; Nieuwpoort-Asquempont Fault Zone of De Vos *et al.*, 1993). André & Deutsch (1985) tentatively attributed the fault contact at the NE-side of the plug to this fault zone. Because of the presumed lateral displacement along part of this fault zone at Bierghes, a lateral displacement was

proposed for the entire fault zone (André & Deutsch, 1985; cf. De Vos *et al.*, 1993), including the fault along the NE-side of the plug at Quenast. More recently, however, Debacker (2001) and Debacker *et al.* (2003, 2004a) demonstrated that the faults of the Nieuwpoort-Asquempont Fault Zone, exposed at Bierghes and in the Senne-Sennette outcrop area, are in fact steeply dipping normal faults. According to these authors, the Nieuwpoort-Asquempont Fault Zone can be regarded as a zone of both N- and S-dipping normal faults, deforming the Lower Palaeozoic basement into a horst-and-graben geometry. A fluid inclusion study of the post-cleavage quartz veins from within the faulted contact zone at the NE-side of the Quenast plug by Dewaele *et al.* (2004) revealed two types of fluids. A first fluid type has a low-salinity H₂O-NaCl-KCl composition, whereas the second fluid type has a high-salinity H₂O-CaCl₂-NaCl composition. According to these authors, fluids of the first type are typically associated with the Nieuwpoort-Asquempont Fault Zone (samples from veins in known normal faults at a.o. Asquempont and Bierghes). The fluid inclusion data from Dewaele *et al.* (2004) thus support the idea that the fault contact at the NE-side of the Quenast plug was active during development of the (normal) Nieuwpoort-Asquempont Fault Zone.

In summary, we propose that the fault contact along the NE-side of the Quenast plug initially formed as a local feature during contractional deformation, and that this contact was later reactivated in a normal fashion during development of the Nieuwpoort-Asquempont Fault Zone. Judging from Rb-Sr isochron ages of André & Deutsch (1985) and outcrop observations, this normal reactivation took place during the Middle and Late Devonian, and likely continued during younger times (Debacker *et al.*, 2003, 2004a). During both periods, the displacement along this fault contact is considered to have been relatively minor.

6.3. The geometry of the plug with respect to the host rocks

As demonstrated (e.g. Fig. 10), the shape of the cleavage trajectories mimics the shape of the plug. In theory, assuming that this happens in three dimensions, it might be possible to estimate the plunge of the plug on the basis of the cleavage orientation in the adjacent incompetent rocks. However, although outcrops Gralex 2 and Gralex 3 show a steeply N- to ENE-dipping cleavage, outcrop Gralex 1 contains a steeply S-dipping cleavage. Possibly, in outcrop Gralex 1 divergent cleavage fanning is responsible for the steeply S-dipping cleavage (cf. Debacker, 2001). Alternatively, cleavage in outcrop Gralex 1 may parallel a local subvertical to steeply S-dipping part of the plug surface. Taking into account the cleavage data, the plug is suggested to be plunging ~60 to 90°NE. This orientation is compatible with the steeply NE-plunging orientation suggested by the hydrothermal alteration zones within the plug (André, pers. comm., 2000).

Because of the pre-kinematic emplacement age of the plug, it is likely that the steeply NE-plunging nature, as inferred above and also suggested by André (pers. comm.,

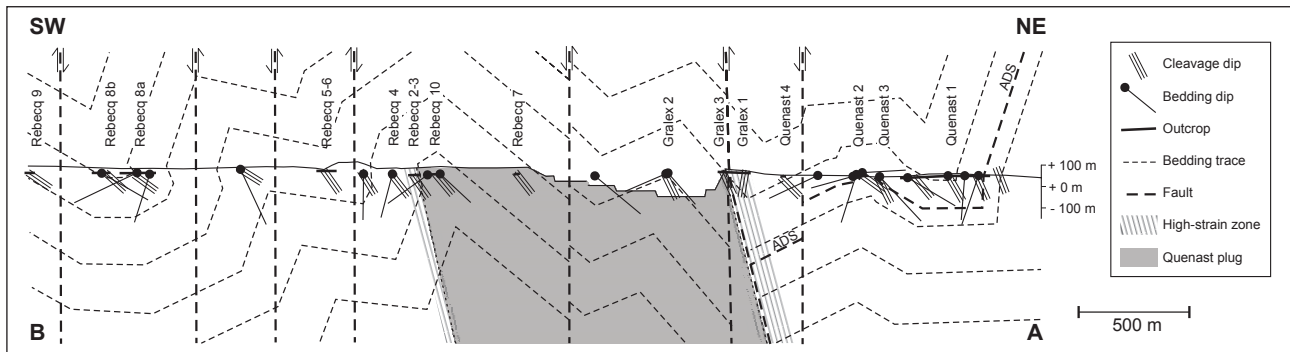


Figure 11 : Schematic section across the Quenast area, based on data of this study, Debacker (2001), Herbosch *et al.* (in press b) and De Meester (2006) (see Fig. 10 for section line). Outcrops to the southwest of Gralex 3 are all situated to the west of the section line. For clarity, these have been projected through the plug. Note that bedding traces on the section do not correspond to formation boundaries. The section is poorly constrained between outcrops Gralex 2 and Rebecq 10 and between Rebecq 4 and Rebecq 8a. In the latter area, the distribution of the different formations suggests important stratigraphic jumps. The majority of these can be explained by step-folds and/or by faults with a down-throw to the southwest, whereas one stratigraphic jump necessitates a fault with a down-throw to the northeast (cf. Herbosch *et al.*, in press b). The likely displacement of the Asquempont Detachment System (ADS) between outcrops Quenast 2 and Quenast 4, is based on the bedding geometry in combination with stratigraphic thicknesses given in Verniers *et al.* (2001).

2000), is not its original orientation. However, given the amount of shortening in the Brabant Massif, and the observations made in this paper, it is unlikely that the Quenast plug experienced a major reorientation and deformation during the Brabantian Orogeny. In our opinion, a tilting of more than 45° , a folding of the plug, or the idea that the plug is actually a strongly tilted sill, is, even on the basis of mechanical and geometrical considerations alone, very unlikely. In order to check this, we made an evaluation of the bedding geometry in the study area. As can be seen on the section in figure 11, across the area, the deposits are folded into a fold train of hectometre-scale, open, SW-verging folds with a predominant step fold geometry, characterised by relatively long straight limbs and rather narrow hinges (cf. Fourmarier, 1921; Lenoir, 1987; De Meester, 2006). This fold train has a gently SW-dipping fold envelope, oriented at high angles to the plug. In addition, the plug is at high angles to the overall bedding in the very well-constrained northeastern section part, where it truncates a gently dipping normal synform limb. Also in the less constrained section part to the southwest of the plug, the plug is at high angles to the overall bedding geometry. To the NW of the plug (“behind” the plug as seen on section), overall bedding geometry is at smaller angles to the plug. However, this part of the section is not very well constrained and, more importantly, these beds are situated next to the plug, and are separated from the plug by –depending on the position– a sinistral detachment and/or low-strain zone (see also Fig. 10). The appearance of the plug at high angles to the fold envelope and to the overall bedding geometry suggests that, initially, the plug was emplaced at high angles to the originally horizontal bedding.

Across the area, cleavage dips less steep than the plug. A steeper cleavage is only observed within the high-strain zone moulding the plug (outcrops Gralex 1 and 3). This is fully compatible with the high competence of the plug. If

the plug was emplaced subperpendicular to bedding, and had the same competence and experienced the same shear strain as the host-rock, its plunge would be comparable to the overall cleavage dip ($\sim 40\text{--}50^\circ\text{NE}$). Its steeper orientation, however, implies much less shear strain than the surrounding host-rocks, this being compatible with its high competence. Probably, the Brabantian deformation event only resulted in a tilting of the plug of maximum 30° .

6.4. The Quenast plug and the Asquempont Detachment System

The upper, exposed part of the Quenast plug is situated in the hanging wall of the Asquempont Detachment System. At a certain depth, estimated at a few hundred meters (see Fig. 11), the plug has to intercept this detachment system. The Asquempont Detachment System is a pre-cleavage low-angle extensional detachment system, which in the Senne area forms the limit between the Lower to lower Middle Cambrian Oisquercq Formation and the Lower Ordovician. At present, its activity can be constrained between the middle Caradoc (Ittre Formation) and the time of cleavage development (Debacker *et al.*, 2003, 2004a, 2005b; Piessens *et al.* 2005; Herbosch *et al.*, in press a). This age interval largely overlaps with the emplacement age of the Quenast plug (U-Pb zircon ages of $433 \pm 10\text{Ma}$; André & Deutsch, 1984). Irrespective of the possible cause of the Asquempont Detachment System, two options exist for the relative timing of plug emplacement and detachment system development. In case the plug pre-dates the Asquempont Detachment System, this would imply that the upper part of the plug was displaced, probably northwards (e.g. Piessens *et al.*, 2005; Herbosch *et al.*, in press a), with respect to the deeper parts of the plug. It is uncertain, however, whether this is mechanically feasible, i.e. whether the detachment system would be capable of cross-cutting and displacing

the Quenast plug, as well as displacing the sills of Lessines (Rb-Sr whole rock ages of 414 ± 16 Ma and 423 ± 33 Ma; André & Deutsch, 1984) and Bierghes, also situated in the detachment hanging wall. The alternative option, in which the plug post-dates the Asquempont Detachment System, would put a more narrow constraint on the timing of the Asquempont Detachment System (between Caradoc and Ludlow, based on absolute age of plug in time scale of Gradstein *et al.*, 2004). In the assumption that the volcanic deposits of the Madot Formation at Fauquez (Ashgill; Van Grootel *et al.*, 1997; Vanmeirhaeghe *et al.*, 2005) are derived from the Quenast plug, this age interval would become even more narrow (Caradoc-Ashgill).

6.5. Amount of cleavage-related shortening?

Across the Brabant Massif, the mean amount of shortening, mainly caused by cleavage development and folding, can be estimated at ~50%. Cleavage development accounts for a shortening of up to ~58% in the Cambrian core (Sintubin *et al.*, 1998) and up to ~45% along the Silurian rim (Debacker *et al.*, 1999). As outlined above, the calculated shortening in the high-strain zone at the NE-side of the plug has a mean value of ~60% (~48% - ~66%), whereas outside the high-strain zone a mean shortening value of ~45% (~36% - ~55%) is obtained. The latter is taken as a regional average for the calculated cleavage-related shortening in the fine-grained deposits in the Quenast area.

As the Quenast plug may be considered as a mega-porphycroclast, a comparison of the amount of shortening of the fine-grained siliciclastic deposits in the Quenast area and the amount of shortening experienced by the plug might be used to deduce the rheological contrast between the plug and the fine-grained siliciclastic host rocks (cf. Treagus & Treagus, 2002). However, determining the amount of shortening experienced by the plug remains problematic. One could attempt to constrain the amount of shortening of the plug by using the cleavage-related amount of shortening in the host rocks, taking into account that the combined effect of shortening across the plug and across the high-strain zone should be equal to the regional shortening. As will become clear, with the present state of knowledge, such an exercise is based on many assumptions, and values should therefore be approached with caution.

If we would assume an originally circular cross-section of the plug, no volume change and no vertical movement of material, the length of the long and short axes of the ellipsoidal plug cross-section could be used to calculate the amount of shortening in a direction subperpendicular to cleavage. This would suggest a shortening of ~13%. As the plug is not subvertical but steeply NE-plunging, the short axis measured is slightly longer than the true short axis oriented perpendicular to the plug axis. This then would result in an amount of shortening that may be as high as ~20%. However, the actual limits of the plug in subcrop are not exactly known and, as pointed out by André (pers. comm., 2007), it is not certain whether the southeastern part of the plug is not a sill rather than a plug (see also André, 1983). Hence, although the results are

geologically feasible, the value of shortening of the plug is much too poorly constrained.

As we made an estimate of the regional amount of shortening due to cleavage development (~45%) and an estimate of the amount of shortening within the high-strain zone (~60%), the amount of shortening of the plug should be a function of the width of the high-strain zone (see appendix). Using the values above, a shortening of the plug by ~20% would imply a high-strain zone of ~900 m wide. A marked bending of the inferred cleavage trajectories occurs up to ~300 m north of the plug, suggesting a similar or smaller width for the high-strain zone. Hence, although also along the southern part of the plug a high-strain zone may occur, the obtained 900 m width is considered too high. Better results for the inferred width of the high-strain zone are obtained by slightly increasing the shortening within the high-strain zone (65%: ~600 m wide high-strain zone), slightly decreasing the regional strain (40%: ~550 m wide high-strain zone) or a combination of both (~400 m wide high-strain zone). Alternatively, when a higher amount of shortening of the plug is allowed for (~25%), a high-strain zone width of ~800 m is obtained using values of ~45% for the regional shortening and ~60% for shortening in the high-strain zone, ~500 m using values of respectively ~45% and ~65%, ~450 m using values of respectively ~40% and ~60%, and ~300 m using values of respectively ~40% and ~65%.

Despite the fact that these data do give an idea about the amount of cleavage-related shortening in the Quenast area, the uncertainty on the values is still too high. The two main uncertainties are the exact thickness of the high-strain zone and the amount of shortening of the Quenast plug. The first problem is difficult to solve, as the high-strain zone is very poorly exposed. The second problem, however, may be addressed by performing magnetic fabric analyses within the quarry. This is currently being undertaken.

7. Conclusion

A number of structural features within the fine-grained siliciclastic host rocks of the Quenast plug indicate a pre-kinematic emplacement age for the Quenast plug, thus being compatible with the observations of Corin (1965) and supporting the radiometric ages of André & Deutsch (1984). These features include a large-scale change in cleavage orientation, a concomitant change in transverse fracture orientation, a related variation in cleavage intensity and degree of preferred phyllosilicate orientation, and the local presence of kink bands and lateral shearing. In combination with the ellipsoidal cross-section of the plug, the Quenast plug may be regarded as having acted as a mega-porphycroclast during the Brabantian deformation event. The majority of the structural features observed can be related to the compression of the fine-grained incompetent host-rock against this competent mega-porphycroclast.

The often frequented northernmost limit of the Quenast

plug, consisting of a quartz vein-bearing fault zone, likely initiated during compressive deformation, and was reactivated as a normal fault as part of the Nieuwpoort-Asquempont Fault Zone (cf. Debacker *et al.*, 2003, 2004a). The proximity to the Asquempont Detachment System, the position of the plug within the hanging wall of this detachment, in combination with the large overlap in age between the emplacement of the plug and the activity of the Asquempont Detachment System has important implications for the origin and evolution of the Asquempont Detachment System within the evolution of the Brabant Basin.

At present, although the amount of shortening in the surroundings of the Quenast plug can be inferred on the basis of a March analysis (March, 1932), the exact amount of shortening of the plug remains unknown. For this purpose, magnetic fabric analyses are proposed and currently being undertaken.

8. Acknowledgements

We kindly acknowledge L. André and J. Bellière for thoroughly reviewing the manuscript. We would like to express our gratitude to A. Vergari and M. Lauwers (Gralex), for the permission to access the quarry, their hospitality and enthusiasm. We would also like to thank A. Herbosch for the helpful field discussions concerning the lithostratigraphical position of the Middle and Upper Ordovician units encountered. T.N. Debacker is a Postdoctoral Fellow of the Fund for Scientific Research-Flanders (F.W.O.-Vlaanderen) and M. Sintubin is a Research Associate of the "Onderzoeksfonds, K.U.Leuven". This work fits into the research projects G.0274.99, G.0094.01 and G.0271.05 of the F.W.O.-Vlaanderen.

Appendix: inferred shortening and width of high-strain zone

The shortening along a given line is given by $(l_0 - l_1)/l_0$, for which l_0 is the original line length and l_1 is the length after shortening (Ramsay & Huber, 1983).

Assuming that the regional amount of shortening in the host-rocks to the SE and NW of the plug_(reg) is identical to the amount of shortening across the plug_(plug) and the high-strain zone along the N-side (and S-side?) of the plug_(strain), it follows that:

$$l_{0(\text{reg})} = l_{0(\text{plug})} + l_{0(\text{strain})}$$

$$l_{1(\text{reg})} = l_{1(\text{plug})} + l_{1(\text{strain})}$$

The latter equation can also be written as:

$$l_{1(\text{reg})} = (1 - e_{(\text{reg})}) l_{0(\text{reg})}$$

for which $e_{(\text{reg})}$ is the regional shortening. Replacing $l_{0(\text{reg})}$ by $l_{0(\text{plug})} + l_{0(\text{strain})}$ results in:

$$l_{1(\text{reg})} = (1 - e_{(\text{reg})}) (l_{0(\text{plug})} + l_{0(\text{strain})})$$

or:

$$l_{1(\text{reg})} = (1 - e_{(\text{reg})}) [l_{1(\text{plug})}/(1 - e_{(\text{plug})}) + l_{1(\text{strain})}/(1 - e_{(\text{strain})})].$$

In the latter equation, $e_{(\text{reg})}$ and $e_{(\text{strain})}$ are deduced from the X-ray pole figure goniometry results by means of a March analysis. $l_{1(\text{plug})}$ can be measured on the map, taking

into account also the steep NE-plunge of the plug. Hence, only $e_{(\text{plug})}$ and $l_{1(\text{strain})}$ remain unknown. A geologically feasible value for $e_{(\text{plug})}$ might be deduced from the ellipsoidal shape of the plug, in the assumption, however, of an initially circular cross-section. Alternatively, for this parameter, alternative strain estimates within the plug may be considered (such as the anisotropy of magnetic susceptibility), or both maximum and minimum estimates might be used in the formula. If successful, only $l_{1(\text{strain})}$ remains truly unknown. This term can be replaced by: $l_{1(\text{reg})} - l_{1(\text{plug})}$ and the resulting equation can then be solved for $l_{1(\text{reg})}$:

$$l_{1(\text{reg})} = [(1 - e_{(\text{reg})}) l_{1(\text{plug})}/(1 - e_{(\text{plug})}) - (1 - e_{(\text{reg})}) l_{1(\text{plug})}/(1 - e_{(\text{strain})})]/[(1 - e_{(\text{reg})})/(1 - e_{(\text{strain})}) - 1]$$

The width of the high-strain zone is given by: $l_1(\text{strain}) = l_1(\text{reg}) - l_1(\text{plug})$

References

- ANDERSON, T. B., 1964. Kink-bands and related geological structures. *Nature* **202**, 272-274.
- ANDRÉ, L., 1983. *Origine et évolution des roches éruptives du Massif du Brabant (Belgique)*. Unpublished Ph.D.-thesis, Free University of Brussels.
- ANDRÉ, L., 1991a. The concealed crystalline basement in Belgium and the "Brabantia" microplate concept: constraints from the Caledonian magmatic and sedimentary rocks. *Annales de la Société Géologique de Belgique* **114**, 117-139.
- ANDRÉ, L., 1991b. Caledonian magmatism. *Annales de la Société Géologique de Belgique* **114**, 315-323.
- ANDRÉ, L. & DEUTSCH, S., 1984. Les porphyres de Quenast et de Lessines: géochronologie, géochimie isotopique et contribution au problème de l'âge du socle Précambrien du Massif du Brabant (Belgique). *Bulletin de la Société belge de Géologie* **93**, 375-384.
- ANDRÉ, L. & DEUTSCH, S., 1985. Very low-grade metamorphic Sr isotopic resettings of magmatic rocks and minerals: Evidence for a late Givetian strike-slip division of the Brabant Massif, Belgium. *Journal of the Geological Society, London* **142**, 911-923.
- ANDRÉ, L. & DEUTSCH, S., 1986. Magmatic Sr-87 Sr-86 relicts in hydrothermally altered quartz diorites (Brabant Massif, Belgium) and the role of epidote as a Sr filter. *Contributions to Mineralogy and Petrology* **92**, 104-112.
- BROWN, E.H. & McCLELLAND, W.C. 2000. Pluton emplacement by sheeting and vertical ballooning in part of the southeast Coast Plutonic Complex, British Columbia. *Geological Society of America Bulletin* **112**, 708-719.
- CECYS, A. & BENN, K. 2007. Emplacement and deformation of the ca. 1.45 Ga Karlshamn granitoid pluton, southeastern Sweden, during ENE-WSW Danopolonian shortening. *International Journal of Earth Sciences* **96**, 397-414.

- COBBOLD, P.R., COSGROVE, J.W. & SUMMERS, J.M., 1971. Development of internal structures in deformed anisotropic rocks. *Tectonophysics* **12**, 23-53.
- CORIN, F., 1965. Atlas des roches éruptives de Belgique. *Mémoires pour servir à l'Explication des Cartes géologiques et minières de la Belgique* **4**, 1-190.
- CZECK, D.M., MAES, S.M., STURM, C.L. & FEIN, E.M., 2006. Assessment of the relationship between emplacement of the Algoman plutons and regional deformation in the Rainy Lake region, Ontario. *Canadian Journal of Earth Sciences* **43**, 1653-1671.
- DAVIS, B.K. & HENDERSON, R.A., 1999. Syn-orogenic extensional and contractional deformation related to granite emplacement in the northern Tasman Orogenic Zone, Australia. *Tectonophysics* **305**, 453-475.
- DEBACKER, T.N., 1999. Folds trending at various angles to the transport direction in the Marcq area, Brabant Massif, Belgium. *Geologica Belgica* **2**, 159-172.
- DEBACKER, T.N., 2001. *Palaeozoic deformation of the Brabant Massif within eastern Avalonia: how, when and why?* Unpublished Ph.D.-thesis, Laboratorium voor Paleontologie, Universiteit Gent.
- DEBACKER, T.N., DEWAELE, S., SINTUBIN, M., VERNIERS, J., MUCHEZ, PH. & BOVEN, A., 2005a. Timing and duration of the progressive deformation of the Brabant Massif, Belgium. *Geologica Belgica* **8**, 20-34.
- DEBACKER, T.N., HERBOSCH, A. & SINTUBIN, M., 2005b. The supposed thrust fault in the Dyle-Thyle outcrop area (southern Brabant Massif, Belgium) re-interpreted as a folded low-angle extensional detachment. *Geologica Belgica* **8**, 53-69.
- DEBACKER, T.N., HERBOSCH, A., SINTUBIN, M. & VERNIERS, J., 2003. Palaeozoic deformation history of the Asquempont-Virginal area (Brabant Massif, Belgium). *Memoirs of the Geological Survey of Belgium* **49**, 30 p.
- DEBACKER, T.N., HERBOSCH, A., VERNIERS, J. & SINTUBIN, M., 2004a. Faults in the Asquempont area, southern Brabant Massif, Belgium. *Netherlands Journal of Geosciences/Geologie en Mijnbouw* **83**, 49-65.
- DEBACKER, T.N., ROBION, P. & SINTUBIN, M., 2004c. The anisotropy of magnetic susceptibility (AMS) in low-grade, cleaved pelitic rocks: influence of cleavage/bedding angle and type and relative orientation of magnetic carriers. In: *Magnetic Fabric: Methods and Applications* (Martin-Hernandez, F., Lüneburg, C.M., Aubourg, C. & Jackson, M. Eds.). Geological Society, London, Special Publications **238**, 77-107.
- DEBACKER, T.N., SINTUBIN, M. & VERNIERS, J., 1999. Cleavage/fold relationships in the Silurian metapelites, southeastern Anglo-Brabant fold belt (Ronquières, Belgium). *Geologie & Mijnbouw* **78**, 47-56.
- DEBACKER, T.N., SINTUBIN, M. & VERNIERS, J., 2001. Large-scale slumping deduced from structural and sedimentary features in the Lower Palaeozoic Anglo-Brabant fold belt, Belgium. *Journal of the Geological Society, London* **158**, 341-352.
- DEBACKER, T.N., SINTUBIN, M. & VERNIERS, J., 2004b. Transitional geometries between gently plunging and steeply plunging folds: an example from the Lower Palaeozoic Brabant Massif, Anglo-Brabant deformation belt, Belgium. *Journal of the Geological Society, London* **161**, 641-652.
- DE COLLEGNO, P., 1835. Séance du 18 mai 1835. Extrait d'un mémoire inédit de M. De Collegno, communiqué par M. Elie de Beaumont. *Bulletin de la Société géologique de France (1ère série)* **6**, 272-275.
- DE LA VALLÉE-POUSSIN, C. & RENARD, A.S.J., 1876. *Mémoire sur les caractères minéralogiques et stratigraphiques des roches dites plutoniques de la Belgique et de l'Ardenne française*. F. Hayez, Bruxelles.
- DE MEESTER, E., 2006. *Studie van plooiën in de Abbaye de Villers Formatie, te Quenast, Senne-vallei (Massief van Brabant, België)*. Unpublished report UGent.
- DENNIS, J.G., 1967. *International tectonic dictionary, English terminology*. A.A.P.G., Tulsa, Oklahoma.
- DE VOS, W., VERNIERS, J., HERBOSCH, A. & VANGUESTAINE, M., 1993. A new geological map of the Brabant Massif, Belgium. *Geological Magazine* **130**, 605-611.
- DEWAELE, S., MUCHEZ, PH. & BANKS, D.A., 2004. Fluid evolution along multistage composite fault systems at the southern margin of the Lower Palaeozoic Anglo-Brabant fold belt, Belgium. *Geofluids* **4**, 341-356.
- DEWEY, J. F., 1965. Nature and origin of kink-bands. *Tectonophysics* **1**, 459-494.
- DUMONT, A., 1848. Mémoire sur les terrains ardennais et rhénan de l'Ardenne, du Rhin, du Brabant et du Condros: seconde partie: terrain rhénan. *Mémoires de l'Académie royale de la Belgique, Classe des Sciences* **22**, 1-451.
- FOURMARIER, P., 1921. La tectonique du Brabant et des régions voisines. *Mémoires de l'Académie royale de la Belgique, Classe Sciences (2è sér.)* **4**, 1-95.
- GALEOTTI, 1835. Aperçu géologique du Brabant méridional. Séance du 18 mai 1835. Extrait du Mémoire sur la Constitution géognostique de la province du Brabant (ouvrage couronné par l'Académie royale des sciences et belles-lettres de Bruxelles, dans la séance du 7 mai 1835). *Bulletin de la Société géologique de France (1ère série)* **6**, 264-272.
- GRADSTEIN, F.M. & OGG, J.G., 1996. A Phanerozoic time scale. *Episodes* **19**, 3-6.
- GRADSTEIN, F.M., OGG, J.G. & SMITH, A.G., 2004. *A geological time scale 2004*. Cambridge University Press, Cambridge.
- HERBOSCH, A., 2005. Hospice de Rebecq: une nouvelle Formation dans l'Ordovicien supérieur du Massif du Brabant (Belgique). *Geologica Belgica* **8**, 35-47.
- HERBOSCH, A., DEBACKER T.N. & PIESSENS, K. (in press a). The stratigraphic position of the Cambrian Jodoigne Formation redefined (Brabant Massif, Belgium). *Geologica Belgica*.
- HERBOSCH, A., DUMOULIN, V., BLOCKMANS, S. & DEBACKER, T. (in press b). Carte Rebecq-Ittre n° 39/1-2, Carte géologique de Wallonie, échelle 1/25000. Ministère de la Région Wallonne, Namur.

- JEDWAB, J., 1950. Introduction à l'étude structurale de la microdiorite de Quenast. *Bulletin de la Société belge de Géologie, de Paléontologie et d'Hydrologie* **59**, 225-230.
- LEGRAND, R., 1967. Ronquières. Documents géologiques. *Mémoires pour servir à l'Explication des Cartes Géologiques et Minières de la Belgique* **6**, 1-60.
- LEGRAND, R., 1968. Le Massif du Brabant. *Mémoires pour servir à l'Explication des Cartes Géologiques et Minières de la Belgique* **9**, 1-148.
- LENOIR, J.L., 1987. *Etude cartographique, pétrographique et palynologique de l'Ordovicien inférieur du bassin de la Senne*. Unpublished M.Sc.-thesis, Université Libre de Bruxelles.
- MALAISE, C., 1873. *Description du terrain silurien du centre de la Belgique*. F. Hayez, Bruxelles.
- MAMTANI, M.A. & GREILING, R.O., 2005. Granite emplacement and its relation with regional deformation in the Aravalli Mountain Belt (India) - inferences from magnetic fabric. *Journal of Structural Geology* **27**, 2008-2029.
- MARCH, A., 1932. Mathematische Theorie der Regelung nach der Korngestalt bei affiner Deformation. *Z. Kristal.* **81**, 285-297.
- OERTEL, G., 1983. The relationship of strain and preferred orientation of phyllosilicate grains in rocks. *Tectonophysics* **100**, 413-447.
- PASSCHIER, C.W., TROUW, R.A.J., GOSCOMBE, B., GRAY, D. & KRÖNER, A., 2007. Intrusion mechanisms in a turbidite sequence: the Voetspoor and Doros plutons in NW Namibia. *Journal of Structural Geology* **29**, 481-496.
- PIESSENS, K., DE VOS, W., BECKERS, R., VANCAMPENHOUT, P. & DE CEUKELAIRE, M., 2005. *Project VLA03-1.1: Opmaak van de pre-Krijt subcropkaart van het Massief van Brabant voor invoering in de Databank Ondergrond Vlaanderen*. Eindverslag. Koninklijk Belgische Instituut voor Natuurwetenschappen, Belgische Geologische Dienst, Brussel.
- RAMSAY, J.G. & HUBER, M.I., 1983. *The techniques of modern structural geology: Volume 1: Strain analysis*. Academic Press, London.
- RAMSAY, J.G. & HUBER, M.I., 1987. *The techniques of modern structural geology: Volume 2: Folds and Fractures*. Academic Press, London.
- ROMEO, I., CAPOTE, R., TEJERO, R., LUNAR, R. & QUESADA, C., 2006. Magma emplacement in transpression: The Santa Olalla Igneous Complex (Ossa-Morena Zone, SW Iberia). *Journal of Structural Geology* **28**, 1821-1834.
- SEDGWICK, A. 1835. Remarks on the structure of large mineral masses, and especially on the chemical changes produced in the aggregation of stratified rocks during different periods after their deposition. *Transactions of the Geological Society, London* **3**, 461-486.
- SIDDANS, A.W.B., 1972. Slaty Cleavage-A review of research since 1815. *Earth-Science Reviews* **8**, 205-232.
- SINTUBIN, M., 1994. Textures in shales and slates. In: *Textures of geological materials* (H.J. Bunge, S. Siegesmund, W. Skrotzki & K. Weber, eds), pp. 221-229. DGM Informationsgesellschaft, Verlag.
- SINTUBIN, M., 1997. Cleavage-fold relationships in the Lower Paleozoic Brabant Massif (Belgium). *Aardkundige Mededelingen* **8**, 161-164.
- SINTUBIN, M., 1998. Mica (110) pole figures in support of Marchian behaviour of phyllosilicates during the development of phyllosilicate preferred orientation. *Materials Science Forum* **273-275**, 601-606.
- SINTUBIN, M., BRODKOM, F. & LADURON, D., 1998. Cleavage-fold relationships in the Lower Cambrian Tubize Group, southeast Anglo-Brabant Fold Belt (Lembeek, Belgium). *Geological Magazine* **135**, 217-226.
- SINTUBIN, M., WENK, H.-R. & PHILLIPS, D. S., 1995. Texture development in materials with a platy grain morphology. A comparison between cold pressed Bi2223-powders and experimental and natural phyllosilicate fabrics. *Materials Science and Engineering* **A202**, 157-171.
- SORBY, H.C., 1853. On the origin of slaty cleavage. *New Philosophical Journal* **55**, 137-148.
- SRIVASTAVA, D.C., LISLE, J.R., IMRAN, M. & KANDPAL, R., 1998. The kink-band triangle: a triangular plot for paleostress analysis from kink-bands. *Journal of Structural Geology* **20**, 1579-1586.
- TREAGUS S.H. & TREAGUS J.E., 2002. Studies of strain and rheology of conglomerates. *Journal of Structural Geology* **24**, 1541-1567.
- TURNER, F.J. & WEISS, L.E., 1963. *Structural analysis of metamorphic tectonites*. McGraw-Hill, New York.
- VAN GROOTEL, G., VERNIERS, J., GEERKENS, B., LADURON, D., VERHAEREN, M., HERTOGEN, J. & DE VOS, W., 1997. Timing of subsidence-related magmatism, foreland basin development, metamorphism and inversion in the Anglo-Brabant fold belt. *Geological Magazine* **134**, 607-616.
- VANMEIRHAEGHE, J., STORME, A., VAN NOTEN, K., VAN GROOTEL, G. & VERNIERS, J., 2005. Chitinozoan biozonation and new lithostratigraphical data in the Upper Ordovician of the Fauquez and Asquempont areas (Brabant Massif, Belgium). *Geologica Belgica* **8**, 145-159.
- VERNIERS, J., HERBOSCH, A., VANGUESTAINE, M., GEUKENS, F., DELCAMBRE, B. PINGOT, J.L., BELANGER, I., HENNEBERT, M., DEBACKER, T., SINTUBIN, M. & DE VOS, W., 2001. Cambrian-Ordovician-Silurian lithostratigraphic units (Belgium). *Geologica Belgica* **4**, 5-38.
- VERNIERS, J., VAN GROOTEL, G. & DEBACKER T., 2005. The Upper Ordovician lithostratigraphy and structural architecture of the Fauquez area (Brabant Massif, Belgium). *Geologica Belgica* **8**, 160-175.
- WALCOTT, C.R. & CRAW, D., 1993. Postemplacement deformation of plutons and their metasedimentary host, Mt Dromedary Area, Southern Victoria Land, Antarctica. *New Zealand Journal of Geology and Geophysics* **36**, 487-496.